Starvation of the bacterium *Vibrio atlanticus* induces simultaneous attacks on the dinoflagellate *Alexandrium pacificum*

Jean Luc Rolland[1, 2†*], Estelle Masseret[3], Mohamed Laabir[3], Guillaume Tetreau[4], Benjamin Gourbal[4], Anne Thebault[5], Eric Abadie[6], Alice Rodrigues-Stien[7,8], Carole Veckerlé[7,8], Elodie Servanne-Meunier[1], Delphine Destoumieux-Garzón[1], Arnaud Lagorce[4,9] , Raphaël Lami[7,9].

Affiliations

[1]IHPE, Univ. Montpellier, CNRS, IFREMER, Université de Perpignan Via Domitia, Montpellier, France.

[2]MARBEC, Univ. Montpellier, IRD, IFREMER, CNRS, Sète, France.

[3]MARBEC, Univ. Montpellier, IRD, IFREMER, CNRS, Montpellier, France.

[4]IHPE, Univ Montpellier, CNRS, IFREMER, Université de Perpignan Via Domitia, Perpignan, France

[5]Agence nationale de sécurité sanitaire de l'alimentation, de l'environnement et du travail (ANSES), ANSES-DER 27-31, avenue du Général Leclerc, 94701 Maison-Alfort, France

[6]IFREMER, 9 rue Jean Bertho, 97822, Le port, la Reunion, France

[7]Sorbonne Université, CNRS, LBBM USR3579, Observatoire Océanologique de Banyuls sur Mer, Avenue Pierre Fabre, 66650 Banyuls-sur-Mer, France.

[8]Sorbonne Université, CNRS, Bio2MAR, Observatoire Océanologique de Banyuls sur Mer, Avenue Pierre Fabre, 66650 Banyuls-sur-Mer, France.

[9]These authors contributed equally

[†]Current address

*Corresponding author: Jean Luc.Rolland

Email: Jean.Luc.Rolland@ifremer.fr

ABSTRACT

Phytoplankton serve as a source of nutrients for bacteria in the marine environment. The interactions between algae and bacteria are known to include mutualism, commensalism, competition or antagonism. This occurs in the microenvironment surrounding phytoplankton cells, the phycosphere. An interface rich in nutrients and organic molecules exuded by the cell. Here, based on *in situ* observation and on an *in vitro* interaction study, we report on a novel form of starvation-induced hunting that the cells of selected *Vibrio* species exert on dinoflagellates. The results showed that *Vibrio atlanticus* was capable of attacking and killing the dinoflagellate *Alexandrium pacificum* ACT03. Briefly, the observed mechanism of algal-killing consists of first, the 'immobilization stage' involving the secretion of algicidal metabolites that disrupt the flagella of the algae. The 'attack stage' when *Vibrios* simultaneously surrounds algal cells at high density for a brief period without invading them. Finally, the 'killing stage' induces the lysis and consumption of the dinoflagellates.

By using a combination of biochemical, proteomic, molecular and fluorescence microscopy approaches, we showed that this relationship is not related to the decomposition of algal organic matter, *Vibrio* quorum sensing pathways, toxicity of the algae or pathogenicity of the bacterium but is conditioned by nutrient stress, iron availability and link to the iron-vibrioferrin transport system of *V. atlanticus*. This is the first evidence of a new mechanism that could to be involved in regulating Alexandrium spp. blooms and giving Vibrio a competitive advantage in obtaining nutrients from the environment.

The interaction model we propose here suggests that Vibrio could play a role in regulating the proliferation of Alexandrium spp., giving it a competitive advantage in obtaining nutrients from the environment.

KEYWORDS

Interaction; Bacterium; Alga; Predation; Environment; Iron related predation

49

INTRODUCTION

Harmful algal blooms (HABs) have experienced an increase in their occurrence, intensity, and geographical distribution on a global scale, resulting in adverse environmental, health, and socioeconomic impacts (Marampouti et al., 2021). HABs have a considerable impact on human health as a result of direct exposure to volatile toxins or by toxic seafood consumption (Burkholder et al., 2018). From an ecological point of view, the expansion of HABs can result in the erosion of biodiversity, because they cause massive mortality of marine species and they are generally monospecific in nature (Chai et al., 2020). In coastal areas, understanding the biological interactions that control toxic algal blooms is therefore a major ecological challenge. Among HAB-causing organisms, a number of *Alexandrium* species have been placed on the list of invasive Mediterranean species. Among them, *Alexandrium pacificum* is a flagellated eukaryotic unicellular organism that together with *Alexandrium tamarense* and *Alexandrium fundyense* form the "Alexandrium tamarense" complex responsible for paralytic shellfish poisoning worldwide (Hadjadji et al., 2020). Since 1998, *A. pacificum* (former *A. catenella*) was monitored by the French phytoplankton observation and monitoring network (Rephy) in the Thau lagoon (French Mediterranean) because it produces paralytic shellfish toxins (PSTs) resulting in paralytic shellfish poisoning (PSP) syndrome.

Laania (Laanaia et al., 2013) showed that in Thau lagoon, a water temperature around 20°C for several days and organic and inorganic nutrients in sufficient concentrations are parameters favoring the development of *A. pacificum*, whose massive blooms occur in autumn. Algal blooms are seasonal events resulting in a rapid increase in the concentration of a species of algae in an aquatic environment. Depending on the species of phytoplankton, tolerance to physicochemical parameters varies, which influences when blooms occur (Leblad et al., 2020). Interestingly, although the collapse of phytoplankton blooms has been previously attributed to viruses (Pal et al., 2020), some ecological studies have suggested an important role of algicidal bacteria (Su et al., 2007; Wang et al., 2010). Among them several are belonging to the Vibrio genus (Li et al., 2014; Wang et al., 2020).

Vibrio (class γ-proteobacteria) are common microorganisms in marine systems worldwide (Baker-Austin et al., 2017; Mavian et al., 2020), where they are important components of the food chain, particularly in biodegradation, nutrient regeneration and biogeochemical cycles (Oberbeckmann et al., 2012). Vibrio is one of the most studied bacterial taxa due to their ubiquity in coastal marine systems and their capacity to cause infections in humans and animals, leading sometimes to epizootic or zoonotic epidemics (LeRoux et al., 2015; Mavian et al., 2020). *Vibrio* are extremely adaptable to their environment (Johnson, 2013). The main factors influencing their occurrence and distribution in water are temperature, salinity, nutrient availability (Wang et al., 2020), multiple strategies such as biofilm formation on biotic and abiotic surfaces (Espinoza-Vergara et al., 2020), or interactions with a multitude of other organisms such as eukaryotic predators (Drebes Dörr and Blokesch, 2020) or plankton (Lopez-Joven et al., 2018) are used by *Vibrio* in the environment. There is also evidence that global climate change has increased *Vibrio*-associated illnesses affecting humans and animals (Brumfield et al., 2021; Muhling et al., 2017). However, the drivers and dynamics of *Vibrio* survival and propagation in the marine environment are not yet fully understood.

A substantial number of research articles have highlighted the potential of γ-proteobacteria to exert algicidal activity against dinoflagellates, supporting the hypothesis that γ-proteobacteria such as *Vibrio* play a role in the control of algae blooms *in situ* (Coyne et al., 2022). However, the mechanisms behind *Vibrio*-driven algal lysis in the environment remain to be elucidated. Particularly, it is unclear how in the water column, algicidal compounds secreted by bacteria can concentrate around the algae to exert their lytic effect.

This study aims to describe observations made in the natural environment between Vibrio bacteria and Alexandrium algal blooms, and to determine in vitro the main factors involved in this relationship. Using a combination of biochemical, proteomic, molecular, and fluorescence microscopy approaches, we explored the role of algal toxicity, bacterial pathogenicity and the quorum sensing pathway on

99 this relationship and showed the important role of nutrient stress and the iron uptake pathway in
100 this unique Vibrio/Alexandrium interaction.

101

102 **METHODS**

103 **Quantification of *Alexandrium* algae and *Vibrio* bacteria in the environment by Qpcr.**

104 Seawater samples were collected in the Thau Lagoon (southern France, a shallow Mediterranean
105 ecosystem open to the sea (Abadie et al., 1999), during spring and autumn 2015. Briefly, samples were
106 collected from the subsurface (-50 cm) near an oyster table at a phytoplankton surveillance site (part of the
107 REPHY network, N 43°26.058' and E 003°39.878'). Once a week during spring and autumn 2015, during
108 field sampling campaigns, 20 L of water was filtered on board through a 180 µm pore-size nylon
109 membrane. At the laboratory, according to Lopez-Joven et al. (Lopez-Joven et al., 2018) seawater was
110 fractionated into two size classes as follows: 2 L of the above filtrate was filtered through a 0.8 µm pore-
111 size polycarbonate Whatman Nuclepore membrane to obtain organisms in the 0.8–180 µm range
112 corresponding to plankton-associated *Vibrio* and living *Alexandrium* forms. Then, the filtrate from the 0.8
113 µm membrane was filtered again through a 0.2 µm pore-size polycarbonate Whatman Nuclepore
114 membrane until the membrane was saturated. *Alexandrium* cells, ranging from 25 to 40 µm, belong to the
115 microphytoplankton and are therefore retained in the 0.8–180 µm fraction. Any *Vibrio* cells potentially
116 associated with or attached to *Alexandrium* cells will also be retained in this fraction. *Vibrio* cells are
117 approximately 0.5-0.8 µm-thick. The fraction between 0.2 and 0.8 µm therefore includes the free-living
118 *Vibrio*. The bacterial population collected on 0.8-µm-pore-size filters was designated the particle-
119 associated community, and the population on 0.2-µm-pore-size filters was designated as the free-living
120 community. Membranes (in triplicate) were then conserved in 500 µL of 100% EtOH at -20°C.
121 Environmental DNA (eDNA) was extracted from the MF Millipore membrane using the Macherey-Nagel
122 NucleoSpin Tissue Kit and resuspended in 100 µL of water. The samples were then stored at -20°C after

123 eDNA quantity and purity were assessed using a NanoDrop system (NanoDrop Technologies,
124 Wilmington, DE, USA). PCR amplification reactions were done on a Roche LightCycler 480 Real-Time
125 thermocycler (qPHD platform, University of Montpellier, France).using specific primer pairs (Table 3).
126 Typically, the reactions contained 1 µL of template DNA (the DNA concentration for all samples varied
127 from 1 to 40 µg mL^{-1}), 0.5 µL of each primer (3.33 µM) and 4 µL of reaction mixture (SYBR Green
128 Master Mix) in a total volume of 6 µL. The reaction parameters were as follows: 5 minutes at 95°C (initial
129 denaturation) and 40 cycles of 10 s at 95°C (denaturation), 10 s at the corresponding hybridization
130 temperature (Table 3) and 10 s at 72°C (elongation). Melting curve profiles were generated by increasing
131 the temperature from 65°C to 95°C at 0.5°C s^{-1}. Amplification products were analysed using LightCycler
132 software (Roche Diagnostics). *Vibrio spp*. and *A. pacificum* and *A. tamarense* were quantified by
133 constructing calibration curves based on DNA from the *V. atlanticus* LGP32 reference strain (former *V.*
134 *tasmaniensis* LGP32) and from the *A. pacificum* reference strain (ACT03: *A. catenella* strain isolated form
135 Thau in 2003) and the *A. tamarense* reference strain (ATT07: *A. tamarense* isolated from Thau in 2007)
136 (not shown).
137
138 **Strains and growth conditions**.
139 *Vibrio* strains. Wild-type and isogenic mutants of *Vibrio atlanticus* LGP32 (Table 1) were used in this
140 study. Deletion-mutants included Δ*luxR*, Δ*luxP*, Δ*luxM* and Δ*pvuB* isogenic strains. The Δ*pvuB* mutant
141 was constructed here by allelic exchange as described previously by Le Roux (Le Roux et al., 2007). We
142 also used *V. atlanticus* LGP32 carrying the pSW3654T-GFP plasmid (Le Roux et al., 2007), hereafter
143 referred to as *V. atlanticus* LGP32-GFP. Bacterial strains were grown at 22 ± 1°C in Zobell medium (0, 38
144 µM iron (III)). When needed, 25 µg mL^{-1} chloramphenicol (Cm) was added to cultures of *V. atlanticus*
145 LGP32-GFP (Le Roux et al., 2007).
146 *Phytoplancton strains*. Non-axenic phytoplankton species (Table 2) were grown in batch culture in
147 enriched natural sea water (ENSW, 6,55 µM iron (III)) with a salinity of 36 practical salinity units (PSU)

148 at 22 ± 1°C under cool white fluorescent illumination (100 µmol photons m^{-2} s^{-1}) and a 12 h:12 h
149 light:dark cycle (Harrison et al., 1980). The algae were used for experiments in their exponential growth
150 phase.

151 **Co-culture assay**

152 For each tested phytoplankton species (Table 2), 2.10^4 cells harvested in their exponential growth phase
153 (doubling time between 5 and 7 days) were placed in 20 mL of ENSW medium in a 50 mL suspension
154 culture flask (Cellstar® PS, Greiner bio-one). After incubation for 24 h at 22 ± 1°C under cool white
155 fluorescent illumination, 40 µL of *Vibrio* strains (Table 1) grown for 12, 36, 60 and 156 h in Zobell
156 medium or in Zobell medium supplemented with $Fecl_3$ (6 µM iron (III)) or with H_3BO_3 (0.47 mM) or the
157 corresponding culture supernatant were added to the phytoplankton cells (Table 2). After incubation at 22
158 ± 1°C for 0, 15, 30, 45 and 60 min under cool white fluorescent lights, living, non-swimming, attacked
159 and lysed phytoplankton cells were counted in a sedimentation chamber under an inverted microscope.
160 The number of lysed cells corresponded to phytoplankton cells showing disrupted membranes. Non-
161 swimming algae were not counted as lysed cells. For *Vibrio* analysis, 100 µL of a 1:10 serial dilution
162 mixture in ENSW (from 10^{-2} to 10^{-10}) was plated on *Vibrio* Selective TCBS (thiosulfate-citrate-bile salts-
163 sucrose) agar (in triplicate). After incubation for 24 h at 22 ± 1°C, the number of living *Vibrio* cells was
164 determined by counting colony-forming units (CFUs). The data come from three independent experiments
165 using independent phytoplankton cultures and independent bacterial cultures.
166

167 **Microscope observations**

168 The dynamic of the interaction between *A. pacificum* ACT03 isolated from the French Thau Lagoon,
169 south of France (Laabir et al., 2011) and *V. atlanticus* LGP32, which is an oyster pathogen isolated from
170 the French Atlantic coast (Gay et al., 2004) and present in the Thau Lagoon (Lopez-Joven et al., 2018) was
171 surveyed. As the *A. pacificum* ACT03 strain (table 2) used in the study is not axenic, there is potential for

172 bacteria other than *V. atlanticus* LGP32 to be present in the experiments. To elucidate the interaction
173 without thoroughly accounting for the non-axenic cells, interaction was observed under a Zeiss Axio
174 upright fluorescence microscope equipped with an AxioCamMRm 2 digital microscope camera using *V.*
175 *atlanticus* LGP32 tagged with green fluorescent protein (GFP). Lasers were used at excitation wavelength
176 (λex) 488 nm for GFP (emission wavelengths (λem): 505–530 nm) and λex 532 nm for plankton chloroplasts
177 (λem 560–630 nm). Images were taken sequentially to avoid cross-contamination between fluorochromes.
178 Sequences of images were merged during the *Vibrio-Alexandrium* interaction using ZEN 2012 (blue edition)
179 software. Interaction events between *Vibrio* strains and phytoplankton strains were also observed under a
180 Leica TCS SPE confocal laser scanning system connected to a Leica DM 2500 upright microscope camera
181 (Montpellier RIO Imaging Platform, University of Montpellier, France).

182 **Comparative proteomic analysis**

183 *Vibrio sampling and protein extraction. V. atlanticus* LGP32 was grown for 60 h at 22°C in artificial
184 seawater (high nutrient stress, cond. 1) or 12 h at 22°C in Zobell media (low nutrient stress, cond. 2). After
185 10 min centrifugation at 8000 rpm, crude protein extracts of *V. atlanticus* LGP32 in each culture condition
186 (triplicates) were obtained by sonication on ice at 20% amplitude for 20 s in 200 µL of ice-cold denaturing
187 buffer (7 M urea, 2 M thiourea, 4% CHAPS in 30 mM Tris-HCl, pH 8.5) and clarified by centrifugation at
188 2000 x *g*, 15 min, 4°C. The protein concentration of the supernatant was estimated using the 2D Quant Kit
189 (Cytiva™, MERCK) and samples were stored at -80°C until use.
190

191 *Bi-dimensional gel electrophoresis (2D gel).* Proteins extracts were individually analysed on 2D gel
192 electrophoresis (6 gels per condition each corresponding to different biological replicates). To do so, 100
193 µg of proteins from each extract was added to rehydration buffer (7 M urea, 2 M thiourea, 4% CHAPS, 65
194 mM DTT) for a total volume of 350 µL. They were then individually loaded onto 17 cm isoelectric
195 focusing strips (Bio-Rad) with a stabilized non-linear pH ranging from 3 to 10. Due to the high

196 complexity of the protein profile in the acidic part (left) of the gel pH 3–10 (Fig. S3), we conducted
197 additional 'close-up' analyses in gels using 17 cm isoelectric focusing strips (Bio-Rad) with a narrower,
198 stabilized pH gradient ranging from 4 to 7. Strips were rehydrated passively for 5 h at 22°C, followed by
199 active rehydration for 14 h under a 50 V current at 22°C (to help large proteins enter the strips).
200 Thereafter, isoelectrofocusing was carried out using the following programme: 50 V for 1 h, 250 V for 1
201 h, 8000 V for 1 h and a final step at 8000 V for a total of 140 000 V.h with a slow ramping voltage
202 (quadratic increasing voltage) at each step. Focused proteins were reduced by incubating the strip twice in
203 equilibration buffer (1.5 M Tris, 6 M urea, 2% SDS, 30% glycerol; bromophenol blue, pH 8.8) containing
204 DTT (130 mM) at 55°C. Then, they were alkylated by incubation with equilibration buffer containing
205 iodoacetamide (135 mM) on a rocking agitator (400 rpm) at room temperature protected from light.
206 Proteins were also separated according to their molecular weight (second dimension) on 12%
207 acrylamide/0.32% piperazine diacrylamide gels run at 25 mA per gel for 30 min followed by 75 mA per
208 gel for 8 h using a Protean II XL system (Bio-Rad). Gels were stained using an MS-compatible silver
209 staining protocol and scanned using a ChemiDoc MP Imaging System (Bio-Rad) associated with Image
210 Lab software version 4.0.1 (Bio-Rad).
211
212 *Comparative bioinformatics analysis of 2D gels.* Twelve gels (six per condition) were selected for
213 comparative analysis on PD-Quest v. 7.4.0 (Bio-Rad) to identify changes in protein abundance between
214 the proteomic profiles of *V. atlanticus* LGP32 cultured in contrasting nutrient conditions (ENSW/Zobell).
215 Spots whose mean intensity across six replicates per strain was two times higher or lower than those from
216 the other strain, with a $P < 0.01$ (Mann-Whitney U-test), were considered significantly different in terms of
217 abundance between the two conditions (quantitative difference). Differentially represented spots were then
218 excised from the gels, destained, trypsin-digested and the obtained peptides were identified by tandem
219 mass spectrometry (MS-MS) using the PISSARO platform facility (University of Rouen, France). To
220 identify protein(s) present in each spot, the obtained peptides were compared with *V. atlanticus* LGP32

221 reference genome *(https://vibrio.biocyc.org/)*. The genes whose peptides matched strongly were retrieved
222 and used for an BLASTx query against non-redundant databases to determine the protein identity of the
223 best match. A gene was considered as strongly matched when at least two peptides matched the sequence
224 with a coverage of> 6%. Their theoretical isoelectric point (pI) and molecular weights were also
225 calculated using the Expasy server (https://www.expasy.org/) to compare them with the location of the
226 spot on the gel. Altogether, these complementary analyses made it possible to characterize the protein
227 identity of each spot with confidence.

228

229 **Gene expression analysis**

230 *Vibrio sampling and RNA extraction. V. atlanticus* LGP32 was grown in Zobell media for 36 h and 60 h at
231 22°C (decline phase of growth, nutrient stress) or for 12 h at 22°C (exponential grow phase, poor nutrient
232 stress). Total RNA was isolated from *V. atlanticus* LGP32 using the standard TRIzol method (Invitrogen
233 Life Technologies SAS, Saint-Aubin, France) and then treated with DNase (Invitrogen) to eliminate
234 genomic DNA contamination. After sodium acetate precipitation, the quantity and quality of the total
235 RNA were determined using a NanoDrop spectrophotometer and agarose gel electrophoresis. Following
236 heat denaturing (70°C for 5 minutes), reverse transcription was performed using 1 µg of RNA prepared
237 with 50 ng μL^{-1} oligo-(dT) 12–18 mer in a 20-µL reaction containing 1 mM dNTPs, 1 unit μL^{-1}
238 RNAseOUT and 200 units μL^{-1} Moloney murine leukaemia virus reverse transcriptase (M-MLV RT) in
239 reverse transcriptase buffer, according to the manufacturer's instructions (Invitrogen Life Technologies
240 SAS, Saint-Aubin, France).

241

242 *PCR amplification*. Amplification reactions were analysed using a Roche LightCycler 480 Real-Time
243 thermocycler (Bio-Environnement platform, University of Perpignan, France). In this study, several PCR
244 primer pairs were designed using Primer3 software (optimal primer size: 20 bases; Tm: 60°C; primer

245 GC%: 50; 2GC clamp and product size range: 150–200 bp) and calibrated with *V. atlanticus* LGP32
246 genomic DNA (Table 1). To determine the qPCR efficiency of each primer pair used, standard curves
247 were generated using seven serial dilutions of genomic DNA (10^{-2}, 10^{-3}, 10^{-4}, 10^{-5}, 10^{-5}, 10^{-7} and 10^{-8}) (not
248 shown); the qPCR efficiencies of the tested genes varied between 1.85 and 2.08 (Table 3). For gene
249 expression, reverse transcription was performed with 1 µg of total RNA using random hexamers and
250 SuperScript IV reverse transcriptase (Invitrogen). The total qPCR reaction volume was 10 µL and
251 consisted of 5 µL of cDNA (diluted 1:5), 2.5 µL of SensiFAST SYBR No-ROX Mix (Bioline) and 100
252 nM or 300 nM PCR primer pair (Table 3). The reaction parameters were as follows: 2 min at 95°C (initial
253 denaturation) and 40 cycles of 5 s at 95°C (denaturation), 10 s at 59°C (annealing) and 20 s at 72°C
254 (elongation). The specificity of each PCR was checked by measuring fluorescent signals during melting
255 curve analysis (PCR product heated from 65°C to 95°C continuously and slowly at 0.1°C s^{-1}). Relative
256 expression was calculated by normalization to the expression of two constitutively expressed
257 housekeeping genes, namely, 6PKF (VS_2913) and CcmC (VS_0852), using the delta-delta threshold
258 cycle (ΔΔCt) method(Pfaffl, 2001).

259

260 **Detection of quorum-sensing signalling molecules**.

261 *Vibrio culture.* To detect the QS molecules (AI-2, AI-1 and CAI-1) *V. atlanticus* LGP32 was grown
262 in Zobell media for 12 h (exponential growth phase, control) and 60 h (decline phase of growth, nutrient
263 stress).

264 *AI-2 analysis.* Bioluminescence assay using the QS bioluminescent of *Vibrio campbellii* MM32
265 (*luxN*::Cm, *luxS*::Tn5Kan) was used to detect AI-2 molecules in culture supernatants. Briefly, *Vibrio*
266 cultures were centrifuged at 17,000 x *g* for 10 min, and the resulting supernatants were filtered on 0.22
267 µm. Then 20 µL of the filtrates were mixed with 180 µL of *V. campbellii* MM32 diluted 1:5000 then

268 incubated at 30°C and 100 rpm. Luminescence and cell density (OD620) were collected in triplicate and
269 analysed according to Tourneroche et al.(Tourneroche et al., 2019).
270
271 *AI-1 and CAI-1 extraction and LC-MS analysis.* Chemical analyses were conducted with a Q Exactive
272 Focus Orbitrap System coupled to an Ultimate 3000™ ultrahigh-performance liquid chromatography
273 (UHPLC) system (Thermo Fisher Scientific) according to Rodrigues et al. (Rodrigues et al., 2022).
274 Briefly, ethyl acetate (2 mL) was added into each culture (2 mL). This mixture was shaken overnight at
275 room temperature (150 rpm). The two phases were then separated and the aqueous phase was extracted
276 once again. The two obtained organic phases were pooled and the solvent was evaporated under vacuum.
277 The crude extracts were dissolved in 500 µL LC-MS grade methanol for analysis. The experiments were
278 performed using biological triplicates, each of which was analyzed in triplicate. Analyses of extracts and
279 standards (3 µL injected) were performed in electrospray positive ionization mode in the 50–750 m/z
280 range in centroid mode. The parameters were as follows: spray voltage: 3 kV; sheath flow rate: 75; aux
281 gas pressure: 20; capillary temperature: 350°C; heater temperature: 430°C. The analysis was conducted in
282 Full MS data-dependent MS2 mode (Discovery mode). Resolution was set to 70,000 in Full MS mode,
283 and the AGC (automatic gain control) target was set to $1x10^6$. In MS2, resolution was 17,500, AGC target
284 was set to $2x10^5$, isolation window was 0.4 m/z, and normalized collision energy was stepped to 15, 30
285 and 40 eV. The UHPLC column was a Phenomenex Luna Omega Polar C18 1.6 µm, 150 x 2.1 mm. The
286 column temperature was set to 42°C, and the flow rate was 0.4 mL min^{-1}. The solvent system was a
287 mixture of water (A) with increasing proportions of acetonitrile (B), with both solvents modified with
288 0.1% formic acid. The gradient was as follows: 1% B 3 min before injection, then from 1 to 15 min, a
289 gradient increase of B up to 100% (curve 5), followed by 100% B for 5 min. The flow was injected into
290 the mass spectrometer starting immediately after injection. All data were acquired and processed using
291 FreeStyle 1.5 software (Thermo Fisher Scientific).
292

293 *Chemicals and solvents.* N-acyl-homoserine lactones (AHL) were obtained from Cayman Chemical (Ann
294 Arbor, MI, USA). Stock solutions were obtained by dissolving standards in methanol or dichloromethane
295 (C18-AHL) at a concentration of 1 mg mL^{-1} and stored at -80°C. Standard solutions for UHPLC- high-
296 resolution tandem mass spectrometry (HRMS) analyses were prepared by diluting each individual
297 standard solution with methanol in order to obtain a concentration range from 2000 to 20 ng mL^{-1}. LC-MS
298 grade methanol, acetonitrile and formic acid were purchased from Biosolve (Biosolve Chimie, Dieuze,
299 France), analytical-grade ethyl acetate was obtained from Sigma-Aldrich. Pure water was obtained from
300 Elga Purelab Flex System (Veolia LabWater STI, Antony, France).

301

302 **Nature of lytic compounds secreted by *V. atlanticus* LGP32**.
303 To determine the temperature-sensitivity of the lytic compounds secreted, *V. atlanticus* LGP32 grown for
304 60 h in Zobell media at 22 °C was filtered through a 10 kDa membrane (Amicon® Ultra-4 filter unit).
305 The eluate containing molecules with MW below 10 KDa was then incubated in a water bath at 100°C for
306 30 min. Boiled filtrates (0.1 mL) were subsequently used to inoculate *A. pacificum* (ACT03 strain)
307 cultures, then lytic activity was observed under the Leica TCS SPE confocal laser scanning system. Zobell
308 media with the same treatment was used as control.

309

310 **Statistical analysis.** *Environmental data*. Statistical analyses were performed using R 3.6.3 software. The
311 relationship between *Alexandrium* and *Vibrio* was explored separately in spring and autumn. We used a
312 generalized linear model specifying a Gaussian family. For spring, the dataset for salinity and temperature
313 was complete (14 periods of observation). An influential period was detected and removed from the
314 dataset because no dead *Alexandrium* cells were observed. The effects of explanatory variables such as
315 log10 (Vibrio+1), salinity and temperature were centred, reduced and tested as fixed effects with a linear

316 relationship. Model selection was performed using the Akaike information criterion corrected for small
317 sample size (AIC_c). Models were considered different whenever the difference between their AIC_c value
318 and the lowest AIC_c value (ΔAIC_c) was lower than 2 (Burnham and Anderson, 2002). *Alexandrium*
319 distribution and model residuals were checked for normal distribution assumptions (QQ plot and Shapiro-
320 Wilk test). For autumn, the dataset was complete for 10 periods of observation. Salinity and temperature
321 were missing for three periods. We explored the relationship between *Alexandrium* and *Vibrio* alone using
322 the method detailed above for spring.
323 *In vitro data*. Statistical analyses were performed using one-way ANOVA (analysed by pair) followed by
324 Tukey's test (Statistica 10.0 software, StatSoft, Maison-Alfort, France). *P <0.05, **P <0.01, ***P
325 <0.001

326 **RESULTS**

327 **Concomitant occurrence of *A. pacificum* ACT03, *A. tamarense* ATT07 and free-living *Vibrio spp.* in**
328 **the Thau lagoon**. In the spring and autumn of 2015, in the Thau Lagoon (Fig. 1A), we detected
329 *Alexandrium* algae (*A. pacificum* ACT03 *and A. tamarense* ATT07, both alive and in degraded cell forms)
330 and free-living *Vibrio*, but no plankton-associated *Vibrio* were observed (Fig. 1B, Data S1). Using model
331 selection based on AICc, we found no significant relationship between *Alexandrium* (*A. pacificum*
332 ACT03*, A. tamarense*) and *Vibrio Spp.* abundances in autumn. This result is consistent with the difficulty
333 Vibrio has in growing at temperatures below 20°C and with the many environmental factors that can
334 influence the dynamics of algae proliferation (Laanaia et al., 2013). Interestingly, in spring 2015, the mean
335 densities of all *Alexandrium* cells (degraded and alive) and of free-living *Vibrio* were positively correlated.
336 The lowest AICc was obtained with the model explaining degraded form of *Alexandrium* density based on
337 the free *Vibrio* density (Fig. 1C). Given that, this model is not so different from the model with only the
338 intercept, but better than any other linear combination with other potentially interfering drivers, such as

339 temperature and salinity (Fig. 1D), we searched for evidence of a relationship between *Vibrio* and
340 *Alexandrium* by studying their interaction *in vitro*.
341

342 ***Vibrio atlanticus* LGP32 feeds on *Alexandrium pacificum* ACT03**.
343 To investigate whether *Alexandrium* interacts with *Vibrio*, we incubated in Enriched Natural SeaWater
344 (ENSW) *A. pacificum* ACT03 (2.0 x 10^4 cells) with *V. atlanticus* LGP32 previously grown for 12 hours in
345 Zobell media (initial concentration of 8.8 x 10^7 cells mL^{-1}). In interaction with *V. atlanticus* LGP32, *A.*
346 *pacificum* ACT03 cell abundance decreased significantly from 2.1 10^4 cells mL^{-1} after 1h of exposure to
347 1.1 x 10^4 cells mL^{-1} after 48 h of exposure (Fig. 2A), while the *V. atlanticus* LGP32 concentration grew
348 significantly after 26 h of interaction, reaching a maximum peak density of 7.6 x 10^7 CFU mL^{-1} at 34 h
349 (Fig. 2B). In the control experiment where *A. pacificum* ACT03 was cultured alone in ENSW, the algal
350 concentration remained stable over time (Fig. 2A) and no bacteria were on the corresponding TCBS plates
351 (*Vibrio* selective medium). In the control where *V. atlanticus* LGP32 was grown alone in ENSW, the
352 bacterial concentration decreased from 7.0 × 10^5 CFU/mL after 1 hour of incubation to 1.1 × 10^5 CFU/mL
353 after 48 hours of incubation (Fig. 2B). These results show that the interaction between *V. atlanticus*
354 LGP32 and *A. pacificum* ACT03 leads to a decline in the algal population and promotes the growth of *V.*
355 *atlanticus* LGP32. This suggests that *V. atlanticus* LGP32 is able to feed on *A. pacificum* ACT03.

356 ***V. atlanticus* LGP32 performs attacks on *A. pacificum* ACT03**.
357 Epifluorescence microscopy observation of GFP-labelled *V. atlanticus* LGP32 (previously grow in Zobell
358 medium) in interaction showed that *V. atlanticus* LGP32 cells are capable to simultaneously attacks *A.*
359 *pacificum* ACT03 cells (Fig, 2C and Video 1). The attacks were extremely rapid, with empty thecae (algal
360 envelopes) observed in the medium after less than 60 s (Fig 2D and Video 2). During the attack, *V.*
361 *atlanticus* LGP32 did not invade the algal cell but remained clustered on the cell surface (Fig. 2C).
362

363 **Attack of *A. pacificum* ACT03 is activated by *V. atlanticus* LGP32 starvation.**

364 In 2002, Martin hypothesized that nutritional stress induces bacteria to lyse algae (Martin, 2002). To test
365 this hypothesis, we monitored *V. atlanticus* LGP32 behaviour in response to starvation (Fig. 3). We
366 observed that *V. atlanticus* LGP32 in exponentially growth phase (12 h of culture in Zobell medium, 8.8 x
367 10^7 cells mL^{-1}) did not interact with *A. pacificum* ACT03 cells for the first hour of contact (Fig. 3A, B, C).
368 In contrast, *V. atlanticus* LGP32 in the decline phase (36 h of culture in Zobell medium, 1.3 10^7 cells mL^{-}
369 ^{1}) induced a significant decrease in the number of motile algae cells by 8.9% after 15 min and by 43.3%
370 after 60 min (Fig. 3A). This phenomenon corresponded to the degradation and/or disruption of algal
371 flagella (Video 3). The flagella no longer functioned correctly, which caused irregular swimming of the
372 algae (Video 3, left cell). This was followed by a complete cessation of swimming. When the flagellum
373 detached from the algae (Video 3, right cell), the attack occurred. With starved *V. atlanticus* LGP32 (60 h
374 of culture in Zobell medium, 0.6 10^7 cells mL^{-1}), algae immobilization was fast and significant (91.4% in
375 15 min, Fig. 3A), and algae were attacked individually being targeted by *V. atlanticus* LGP32 cells
376 (Video 4). The percentage of cells attacked and killed peaked at 30% after 15–30 min of contact (Fig. 3B
377 and 3B1) and then decreased. After 1 h, attacks had stopped with approximately 40% of the algal cells still
378 alive (Fig. 3B1 and 3C). Although it remains unclear whether the attacks occur during a specific phase of
379 growth, it is evident that the cells are already weakened before attack as they have all lost their flagella.
380 An old-starved culture of *V. atlanticus* LGP32 (126 h of culture in Zobell medium, < 0.1 10^7 cells mL^{-1})
381 significantly immobilized *A. pacificum* ACT03 cells within a few minutes, with lysis occurring
382 immediately (Fig. 3A and 3C), making it impossible to detect attacks by *V. atlanticus* LGP32 (Fig. 3B).
383 The lysis phase corresponded to initial vesicle formation followed by the bursting of *A. pacificum* ACT03
384 cells (Fig. 3C and 3C1).

385 We next tested whether this lytic effect was linked to *Vibrio* culture supernatant and mediated by
386 thermostable molecule (s) secreted by *Vibrio*. The culture supernatant of starved culture of *V. atlanticus*
387 LGP32 (36 h) filtered through a 10 kDa membrane and then incubated at 100°C for 30 min still possessed

388 its lytic properties, indicating that the algicidal compounds produced by *V. atlanticus* LGP32 are small
389 thermostable molecules unlikely to be lytic enzymes, or lysins able to digest the algae cell. However, these
390 experimental observations clearly show the key role of nutrient limitation in triggering the attack
391 behaviour and the secretion of lytic compounds of *V. atlanticus* LGP32.

392 **Attack occurs on *A. pacificum* ACT03 in exponential phase of growth.**

393 Here, we wondered whether the live/dead status of algae is important for *V. atlanticus* LGP32-mediated
394 attacks targeting. To this end, *A. pacificum* ACT03 in exponential growth phase was first exposed for 30
395 minutes to the supernatant of a 126-hour culture of *V. atlanticus* LGP32, which induced lysis of 70% of
396 the *A. pacificum* ACT03 cells (Figures 3C and 3C1 (arrow 2) and Video 4). Next, cells of *V. atlanticus*
397 LGP32 from a 60-hour culture, capable of attacking *A. pacificum* ACT03 cells (Fig. 3B), were added. For
398 1 hour of exposure, no attack was observed on the previously lysed algae. This result is similar to what is
399 observed on the Video 1 with flash attacks only on immobilized, but not degraded *A. pacificum* ACT03
400 cells (red), and not on lysed cells (green). In addition, no attacks occurred on cells from an old *A.*
401 *pacificum* ACT03 culture (1-month culture). Together, with the very short duration of attacks (Video 1),
402 these results indicate that *V. atlanticus* LGP32 attacked exponentially growing cells of *A. pacificum*
403 ACT03, but not decomposing algae, suggesting that this behaviour is not just an opportunistic response of
404 heterotrophic bacteria to organic substrates.

405

406 **Attack is independent of quorum sensing.**

407 Considering the simultaneous action of *V. atlanticus* LGP32 in attacks on *A. pacificum* ACT03, we tested
408 whether the attack process depended on the key physiological mechanism that regulates many functions in
409 marine microbial cells, quorum sensing (QS) (Lami, 2019; Papenfort and Bassler, 2016), a type of cell-
410 cell communication. Although QS is a cell-density-dependent mechanism, our results showed no attack

411 from a 12 h culture of *V. atlanticus* LGP32 up to a concentration of 4.10^6 *Vibrio* mL^{-1} (Fig 4A). Attacks
412 were only observed with *V. atlanticus* LGP32 from a 60 h culture at low concentration of 5.10^3 *Vibrio* mL^{-}
413 ^{1} to the highest concentration tested of 5.10^5 *Vibrio* mL^{-1} (Fig 4A), consistent with the hypothesis that the
414 attacks were independent of *Vibrio* density.
415 The analysis of the expression of genes involved in the known QS pathways in *Vibrio* cell (Fig. S3A),
416 highlighted that only the AI-2 pathway was induced during nutrient stress of *V. atlanticus* LGP32*,* because
417 only the expression of the AI synthase (*LuxS*) and its receptor (*LuxP*) increased significantly (Fig. 4B;
418 ANOVA $p < 0.05$). This was confirmed by a QS bioluminescence assay, which showed a AI-2 molecules
419 (unquantified) in the Zobell culture supernatant of *V. atlanticus* LGP32 after 60 h of culture but not after
420 12 h of culture and not in the ENSW supernatant of *V. atlanticus* LGP32 after 12 or 60 h of culture.
421 UHPLC-HRMS/MS provided no evidence of detectable HAI-1) and CAI-1 in any experiments.

422 Targeted mutagenesis of key genes involved in two of the three known QS pathways in vibrios (Fig. S3),
423 ΔluxM (HAI-1 production), ΔluxS (AI-2 production), and ΔluxR (main high-density QS regulator), did
424 not result in any changes in the attack behavior of *V. atlanticus* LGP32 (Fig. 4C). Combined with the
425 absence of overexpression of the CqsS gene (inducible by CAI-1) involved in the last known QS pathway
426 in Vibrio (Fig. S3), these results indicated that the attack by *V. atlanticus* LGP32 is most likely unrelated
427 to QS.

428 **Attack related to the availability of iron**.
429 The comparative analysis of the proteome of *V. atlanticus* LGP32 incubated 60 h in artificial seawater
430 (ENSW) versus *V. atlanticus* LGP32 grown 12 h in Zobell nutrient-rich medium revealed 10 proteins
431 modulated by nutrient stress (Fig. S2). The two most down-regulated proteins correspond to be ß-
432 ketoacyl-(acyl-carrier-protein) synthase II (-22-fold in ENSW compared to Zobell), a key regulator of
433 bacterial fatty acid synthesis, and the dihydroorotase (-6.6-fold in ENSW compared to Zobell), an enzyme
434 essential for pyrimidine biosynthesis and thus bacterial proliferation and growth. The low expression of

435 these proteins in ENSW is consistent with *V. atlanticus* LGP32 nutritional starvation. The most up-
436 regulated protein in starved *V. atlanticus* LGP32, with an increase of more than 6-fold, was glucosamine-
437 6-phophate deaminase, an enzyme involved in bacterial energy metabolism probably necessary for its
438 survival. Among the other up -regulated proteins, one was an iron siderophore-binding protein (Spot 4413,
439 Fig. S2A) corresponding to the vibrioferrin outer membrane receptor PvuB, whose gene is part of the *pvu*
440 operons involved in iron transport (Fig. S3B). Interestingly, the corresponding gene *pvuB* as well as the
441 vibrioferrin membrane receptor gene *pvuA2* (Fig. S3B) were both significantly induced in *Vibrio* under
442 nutrient stress (Fig. 4B; ANOVA $p < 0.01$) but not the one involved in the vibrioferrin biosynthesis, *pvsA*
443 (Fig. 4B). Remarkably, among the 10 proteins identified by proteomic analysis only *V. atlanticus* LGP32
444 mutant lacking *pvuB* failed to attack *A. pacificum* ACT03 (Fig. 4C; ANOVA $p < 0.001$). In the absence of
445 the *pvuB* gene, *V. atlanticus* LGP32 was unable to attack simultaneously *A. pacificum* ACT03. In addition,
446 *V. atlanticus* LGP32 cells that had been washed with ENSW to remove their culture supernatant
447 metabolites also failed to attack *A. pacificum* ACT03 (Fig. 4C; ANOVA $p < 0.001$), which is congruent
448 with the hypothesis that attacks depend on the *V. atlanticus* LGP32 vibrioferrin transport system. Finally,
449 attacks increased significantly, when $FeCl_3$ was added to the *Vibrio* culture medium (Fig. 4D) but not with
450 H_3BO_4 (Fig. 4D) Finally, attacks increased significantly, when FeCl3 was added to the Vibrio culture
451 medium but not with H_3BO_4 known also to be capable of being transported by vibrioferrin (see Fig. 4D)..
452 Taken together, those results are consistent with the hypothesis that attacks are regulated by iron.

453 .

454 **Attack is a *Vibrio spp.* behaviour specific to *Alexandrium spp.***

455 To evaluate the dinoflagellates specificity of the attack behaviour, a selection of *Vibrio spp.* was co-
456 cultured with a selection of dinoflagellate strains commonly found in the Mediterranean Sea. The results
457 showed that, among the *Vibrio spp*. tested (pathogenic or not) all, under nutrient stress, were able to
458 secrete algicidal compounds, immobilize, attack and lyse *A. pacificum* ACT03 cells (Table 1) and no

459 linked to their pathogenesis for fish of invertebrates was observed (Table 1). Among the sixteen
460 dinoflagellates species tested, only *Alexandrium spp*. (non-toxic and paralytic shellfish toxin (PST)
461 producers) and *Gymnodinium catenatum* (PST producer) were immobilized, attacked and lysed by *V.*
462 *atlanticus* LGP32 (Table 2), but no linked to PSTs was revealed (Table 2).

463

464 **DISCUSSION**

465 Predation is a widespread mode of interaction for survival in the natural world (Finke and Denno, 2004;
466 Sinclair et al., 2003). Among predators, predatory bacteria are found in a wide variety of environments
467 and, like bacteriophages and predatory protists, feed primarily on other bacteria, although a few cases of
468 predation on microbial eukaryotes have also been reported (Johnke et al., 2014; Perez et al., 2016).
469 Consider a predator as a free-living organism that kills its prey and feeds on it, this study provides data
470 suggesting the ability of Vibrios to develop an original predator-like behaviour to kill and feed on algae.
471

472 In fact, the strategy developed by *Vibrio* to kill algae may be reminiscent of strategies previously
473 described in the prokaryotes (Johnke et al., 2014). As shown in Video 1, the interaction between *V.*
474 *atlanticus* LGP32 and *A. pacificum* ACT03 proceeds in three stages (Fig. 5). The first stage, the
475 '**immobilization stage**', recalls the strategy used by *Streptomyces* to immobilize its prey (Kumbhar et al.,
476 2014) based on the secretion of algicidal metabolites that disrupt the flagella. The second stage, the
477 '**attack stage**' corresponding to the physical contact between Vibrios and Alexandrium, is similar to the
478 strategy used by *Myxococcus xanthus* and Lysobacter. These bacteria must be in close proximity to their
479 prey in order to cause lysis and utilize their biomass, regardless of the prey's species (Martin, 2002;
480 Genovesi et al., 2013; Perez et al., 2016; Zhang et al., 2020). *V. atlanticus* LGP32 also surrounds *A.*
481 *pacificum* ACT03 cells at high density for a very short time, but does not invade the algal cell. Visually,
482 this phenomenon resembles bacteria clustering around lysed ciliate cells (Blackburn et al., 1998). The

483 third stage, the '**killing stage**', is similar to that of epibiotic bacterial predators, which induces the lysis of
484 bacteria from the outside (Rashidan and Bird, 2001). Overall, these observations suggest that *V. atlanticus*
485 LGP32 can exhibit a predator-like behaviour.
486
487 The attack behaviour of *V. atlanticus* LGP32 was linked to iron absorption, as mutants with impaired iron
488 absorption completely lost its ability to attack the algae. Iron is an essential element for growth in most
489 organisms, including phytoplankton (Martin and Fitzwater, 1988) and bacteria (Neilands, 1981), and its
490 concentration in seawater is known to be very low with measurements in the open ocean surface at 0.2 nM
491 and in deep waters at 0.6 nM (Millero, 1998).

492 Moreover, Its low solubility in seawater limits its availability (Bruland et al., 1994; Wu and Luther, 1994).
493 To acquire iron, bacteria have developed systems based on the secretion (and subsequent uptake) of iron-
494 chelating siderophores to obtain this element from the environment (Amin et al., 2009a). Therefore, many
495 *Vibrio spp*. produce a siderophore known as vibrioferrin, which is synthesized and secreted by proteins
496 encoded by the *pvsABCDE* gene cluster (Fig. S3). Given that boron is known for its role in regulating a
497 global bacterial cellular response to phytoplankton and to bind to vibrioferrin (Romano et al., 2013;
498 Weerasinghe et al., 2013), we tested its potential involvement in simultaneous vibrio attacks. Compared to
499 the Zobell control, no effect on the number of attacks was observed. For iron-vibrioferrin uptake, *Vibrio*
500 *parahaemolyticus* uses a membrane siderophore receptor, called PvuA, which is coupled to an inner
501 membrane ATP-binding cassette (ABC). This ABC transporter system comprised of proteins encoded by
502 the pvuABCDE gene cluster (Fig. S3) is required for transporting the siderophore across the inner
503 membrane (Tanabe et al., 2003). Siderophores are not only iron carriers but also important regulators of
504 virulence (Miethke and Marahiel, 2007) and mediators of bacterial interaction with phytoplankton (Amin
505 et al., 2009b; Kramer et al., 2020). We showed here a pivotal role of iron in the interaction between *V.*
506 *altlanticus* LGP32 and *A. pacificum* ACT03. This mirrors the mutualistic interaction observed between

507 *Gymnodinium catenatum* and *Marinobacter* (Amin et al., 2009b). In fact, in natural settings, the co-
508 occurence of *Marinobacter* and *G. catenatum* is suggested to depend on a mutually beneficial utilization
509 of iron and carbon resources (Bolch et al., 2011). As in the present study, iron seems to play a key role in
510 the interaction. Indeed, the labile iron released through the photolysis of ferric chelates with vibrioferrin
511 providing a crucial iron source for phytoplankton, which need substantial amounts of iron to support
512 carbon fixation through photosynthesis (Amin et al., 2009a; Yang et al., 2021). This fixed carbon, in turn,
513 sustains the growth of both the phytoplankton and their bacterial counterparts (Amin et al., 2009b; Kramer
514 et al., 2020). Interestingly, if a general nutrient deficiency causes attacks, iron supplementation increases
515 this number of attacks (Figure 4D), suggesting the importance of iron absorption in the attack behavior.
516 Future studies should determine whether nutrient deficiency increases the iron absorption capacity of
517 Vibrio bacteria and whether this could plays a major role in the attack mechanism.
518
519 This study showed that quorum sensing is not involved in microbial attacks. Thus, *Vibrio atlanticus*
520 LGP32 mutants lacking the genes involved in known quorum sensing pathways exhibit the same
521 phenotype as wild-type *Vibrio atlanticus* LGP32, and Vibrio density does not induce attacks. However, V.
522 atlanticus LGP32 produces AI-2 during attacks. Quorum sensing and iron acquisition are sometimes
523 interconnected in Vibrio (McRose et al., 2018). For example, in *Vibrio vulnificus*, the production of
524 vulnibactin (a siderophore) is known to be controlled by AI-2 (Kim and Shin, 2011). Similarly, AI-2 could
525 be involved in the production of vibriferin in *Vibrio atlanticus* LGP32.

526 In the natural environment, associations between bacteria and algae have already been observed (Lopez-
527 Joven et al., 2018; Miller et al., 2005; Rosales et al., 2022; Xu et al., 2022). We have shown here that algal
528 attacks by vibrios can be carried out in vitro. Environnemental data collected in the Thau lagoon showed a
529 correlation between the presence of Alexandrium and that of Vibrio, suggesting that such interactions
530 could also occur in the marine environnement. If that were the case, this behaviour would provide an

important ecological advantage to *Vibrio* to obtain nutrients in environment, where *Alexandrium spp*. and *Gymnodinium catenatum* form blooms.

With more than 30 species distributed all over the world (Anderson et al., 2012; Hallegraeff et al., 2021), *Alexandrium spp.* and *Gymnodinium spp*. considered as invasive species by the Delivering Alien Invasive Species Inventories for Europe (http://www.europe-aliens.org)), could play an unexpected and important role in maintaining, structuring and regulating *Vibrio* populations in the ecosystem. In turn, *Vibrio* could contribute to the regulation and control of their blooms.

To conclude, this study reveals the capacity of some *Vibrio spp*. to be facultative predators-like that hunt specific algae. In the current context of climate change favourable to their development monitoring the invasive algae, *Alexandrium spp*. and *Gymnodinium catenatum* should be considered not only for their potent harmful effect on humans and animals, but also as a potential source of nutrients for the expansion of *Vibrio*, particularly pathogenic species (Lemire et al., 2015).

DATA AVAILABILITY

All data on environmental study are included in the article and/or supporting information files. All other study data are available on request from the corresponding author.

REFERENCES

Abadie, E., Amzil, Z., Belin, C., Comps, M.A., Elzière-Papayanni, P., Lassus, P., le Bec, C., Baut, M.L., Nezan, E., Poggi, R., 1999. Contamination de l'étang de Thau par Alexandrium tamarense (No. Rapport 884). Ifremer.

Abadie, E., Kaci, L., Berteaux, T., Hess, P., Sechet, V., Masseret, E., Rolland, J.L., Laabir, M., 2015. Effect of Nitrate, Ammonium and Urea on Growth and Pinnatoxin G Production of Vulcanodinium rugosum. Mar. Drugs 13, 5642–5656. https://doi.org/10.3390/md13095642

Amin, S.A., Green, D.H., Hart, M.C., Kuepper, F.C., Sunda, W.G., Carrano, C.J., 2009a. Photolysis of iron-siderophore chelates promotes bacterial-algal mutualism. Proc. Natl. Acad. Sci. U. S. A. 106, 17071–17076. https://doi.org/10.1073/pnas.0905512106

Amin, S.A., Green, D.H., Kuepper, F.C., Carrano, C.J., 2009b. Vibrioferrin, an Unusual Marine Siderophore: Iron Binding, Photochemistry, and Biological Implications. Inorg. Chem. 48, 11451–11458. https://doi.org/10.1021/ic9016883

Anderson, D.M., Alpermann, T.J., Cembella, A.D., Collos, Y., Masseret, E., Montresor, M., 2012. The globally distributed genus Alexandrium: Multifaceted roles in marine ecosystems and impacts on human health. Harmful Algae 14, 10–35. https://doi.org/10.1016/j.hal.2011.10.012

Baker-Austin, C., Trinanes, J., Gonzalez-Escalona, N., Martinez-Urtaza, J., 2017. Non-Cholera Vibrios: The Microbial Barometer of Climate Change. Trends Microbiol. 25, 76–84. https://doi.org/10.1016/j.tim.2016.09.008

Ben-Gharbia, H., Yahia, O.K.-D., Amzil, Z., Chomerat, N., Abadie, E., Masseret, E., Sibat, M., Triki, H.Z., Nouri, H., Laabir, M., 2016. Toxicity and Growth Assessments of Three Thermophilic Benthic Dinoflagellates (Ostreopsis cf. ovata, Prorocentrum lima and Coolia monotis) Developing in the Southern Mediterranean Basin. Toxins 8, 297. https://doi.org/10.3390/toxins8100297

Blackburn, N., Fenchel, T., Mitchell, J., 1998. Microscale nutrient patches in planktonic habitats shown by chemotactic bacteria. Science 282, 2254–2256. https://doi.org/10.1126/science.282.5397.2254

Bolch, C.J.S., Subramanian, T.A., Green, D.H., 2011. THE TOXIC DINOFLAGELLATE *GYMNODINIUM CATENATUM* (DINOPHYCEAE) REQUIRES MARINE BACTERIA FOR GROWTH[1]. J. Phycol. 47, 1009–1022. https://doi.org/10.1111/j.1529-8817.2011.01043.x

Bruland, K., Orians, K., Cowen, J., 1994. Reactive Trace-Metals in the Stratified Central North Pacific. Geochim. Cosmochim. Acta 58, 3171–3182. https://doi.org/10.1016/0016-7037(94)90044-2

Brumfield, K.D., Usmani, M., Chen, K.M., Gangwar, M., Jutla, A.S., Huq, A., Colwell, R.R., 2021. Environmental parameters associated with incidence and transmission of pathogenic *Vibrio spp* . Environ. Microbiol. 23, 7314–7340. https://doi.org/10.1111/1462-2920.15716

Burkholder, J.M., Shumway, S.E., Glibert, P.M., 2018. Food Web and Ecosystem Impacts of Harmful Algae, in: Harmful Algal Blooms. John Wiley & Sons, Ltd, pp. 243–336. https://doi.org/10.1002/9781118994672.ch7

Burnham, K.P., Anderson, D.R. (Eds.), 2002. Summary, in: Model Selection and Multimodel Inference: A Practical Information-Theoretic Approach. Springer, New York, NY, pp. 437–454. https://doi.org/10.1007/978-0-387-22456-5_8

Chai, Z.Y., Wang, H., Deng, Y., Hu, Z., Tang, Y.Z., 2020. Harmful algal blooms significantly reduce the resource use efficiency in a coastal plankton community. Sci. Total Environ. 704, 135381. https://doi.org/10.1016/j.scitotenv.2019.135381

Coyne, K.J., Wang, Y., Johnson, G., 2022. Algicidal Bacteria: A Review of Current Knowledge and Applications to Control Harmful Algal Blooms. Front. Microbiol. 13, 871177. https://doi.org/10.3389/fmicb.2022.871177

Drebes Dörr, N.C., Blokesch, M., 2020. Interbacterial competition and anti-predatory behaviour of environmental *Vibrio cholerae* strains. Environ. Microbiol. 22, 4485–4504. https://doi.org/10.1111/1462-2920.15224

Espinoza-Vergara, G., Hoque, M.M., McDougald, D., Noorian, P., 2020. The Impact of Protozoan Predation on the Pathogenicity of Vibrio cholerae. Front. Microbiol. 11, 17. https://doi.org/10.3389/fmicb.2020.00017

Fertouna-Bellakhal, M., Dhib, A., Fathalli, A., Bellakhal, M., Chomérat, N., Masseret, E., Laabir, M., Turki, S., Aleya, L., 2015. Alexandrium pacificum Litaker sp. nov (Group IV): Resting cyst distribution and toxin profile of vegetative cells in Bizerte Lagoon (Tunisia, Southern Mediterranean Sea). Harmful Algae 48, 69–82. https://doi.org/10.1016/j.hal.2015.07.007

Finke, D.L., Denno, R.F., 2004. Predator diversity dampens trophic cascades. Nature 429, 407–410. https://doi.org/10.1038/nature02554

Gay, M., Renault, T., Pons, A.M., Le Roux, F., 2004. Two Vibrio splendidus related strains collaborate to kill Crassostrea gigas: taxonomy and host alterations. Dis. Aquat. Organ. 62, 65–74. https://doi.org/10.3354/dao062065

Genovesi, B., Mouillot, D., Laugier, T., Fiandrino, A., Laabir, M., Vaquer, A., Grzebyk, D., 2013. Influences of sedimentation and hydrodynamics on the spatial distribution of Alexandrium catenella/tamarense resting cysts in a shellfish farming lagoon impacted by toxic blooms. Harmful Algae 25, 15–25. https://doi.org/10.1016/j.hal.2013.02.002

Genovesi, B., Shin-Grzebyk, M.-S., Grzebyk, D., Laabir, M., Gagnaire, P.-A., Vaquer, A., Pastoureaud, A., Lasserre, B., Collos, Y., Berrebi, P., Masseret, E., 2011. Assessment of cryptic species diversity within blooms and cyst bank of the Alexandrium tamarense complex (Dinophyceae) in a Mediterranean lagoon facilitated by semi-multiplex PCR. J. Plankton Res. 33, 405–414. https://doi.org/10.1093/plankt/fbq127

Hadjadji, I., Laabir, M., Frihi, H., Collos, Y., Shao, Z.J., Berrebi, P., Abadie, E., Amzil, Z., Chomérat, N., Rolland, J.L., Rieuvilleneuve, F., Masseret, E., 2020. Unsuspected intraspecific variability in the toxin production, growth and morphology of the dinoflagellate Alexandrium pacificum R.W. Litaker (Group IV) blooming in a South Western Mediterranean marine ecosystem, Annaba Bay (Algeria). Toxicon 180, 79–88. https://doi.org/10.1016/j.toxicon.2020.04.005

Hallegraeff, G.M., Anderson, D.M., Belin, C., Bottein, M.-Y.D., Bresnan, E., Chinain, M., Enevoldsen, H., Iwataki, M., Karlson, B., McKenzie, C.H., Sunesen, I., Pitcher, G.C., Provoost, P., Richardson, A., Schweibold, L., Tester, P.A., Trainer, V.L., Yñiguez, A.T., Zingone, A., 2021. Perceived global increase in algal blooms is attributable to intensified monitoring and emerging bloom impacts. Commun. Earth Environ. 2, 117. https://doi.org/10.1038/s43247-021-00178-8

Harrison, P., Waters, R., Taylor, F., 1980. A Broad-Spectrum Artificial Seawater Medium for Coastal and Open Ocean Phytoplankton. J. Phycol. 16, 28–35. https://doi.org/10.1111/j.1529-8817.1980.tb00724.x

Johnke, J., Cohen, Y., de Leeuw, M., Kushmaro, A., Jurkevitch, E., Chatzinotas, A., 2014. Multiple micro-predators controlling bacterial communities in the environment. Curr. Opin. Biotechnol. 27, 185–190. https://doi.org/10.1016/j.copbio.2014.02.003

Johnson, C.N., 2013. Fitness Factors in Vibrios: a Mini-review. Microb. Ecol. 65, 826–851. https://doi.org/10.1007/s00248-012-0168-x

Kim, C.M., Shin, S.H., 2011. Modulation of Iron-Uptake Systems by a Mutation of luxS Encoding an Autoinducer-2 Synthase in Vibrio vulnificus. Biol. Pharm. Bull. 34, 632–637. https://doi.org/10.1248/bpb.34.632

Kitatsukamoto, K., Oyaizu, H., Nanba, K., Simidu, U., 1993. Phylogenetic-Relationships of Marine-Bacteria, Mainly Members of the Family Vibrionaceae, Determined on the Basis of 16s Ribosomal-Rna Sequences. Int. J. Syst. Bacteriol. 43, 8–19. https://doi.org/10.1099/00207713-43-1-8

Kramer, J., Oezkaya, O., Kuemmerli, R., 2020. Bacterial siderophores in community and host interactions. Nat. Rev. Microbiol. 18, 152–163. https://doi.org/10.1038/s41579-019-0284-4

Kumbhar, C., Mudliar, P., Bhatia, L., Kshirsagar, A., Watve, M., 2014. Widespread predatory abilities in the genus Streptomyces. Arch. Microbiol. 196, 235–248. https://doi.org/10.1007/s00203-014-0961-7

Laabir, M., Jauzein, C., Genovesi, B., Masseret, E., Grzebyk, D., Cecchi, P., Vaquer, A., Perrin, Y., Collos, Y., 2011. Influence of temperature, salinity and irradiance on the growth and cell yield of the

harmful red tide dinoflagellate Alexandrium catenella colonizing Mediterranean waters. J. Plankton Res. 33, 1550–1563. https://doi.org/10.1093/plankt/fbr050

Laanaia, N., Vaquer, A., Fiandrino, A., Genovesi, B., Pastoureaud, A., Cecchi, P., Collos, Y., 2013. Wind and temperature controls on Alexandrium blooms (2000-2007) in Thau lagoon (Western Mediterranean). Harmful Algae 28, 31–36. https://doi.org/10.1016/j.hal.2013.05.016

Labreuche, Y., Le Roux, F., Henry, J., Zatylny, C., Huvet, A., Lambert, C., Soudant, P., Mazel, D., Nicolas, J.-L., 2010. Vibrio aestuarianus zinc metalloprotease causes lethality in the Pacific oyster Crassostrea gigas and impairs the host cellular immune defenses. Fish Shellfish Immunol. 29, 753–758. https://doi.org/10.1016/j.fsi.2010.07.007

Lami, R., 2019. Quorum Sensing in Marine Biofilms and Environments, in: Quorum Sensing, Academic Press. Elsevier, pp. 55–96. https://doi.org/10.1016/B978-0-12-814905-8.00003-4

Le Roux, F., Binesse, J., Saulnier, D., Mazel, D., 2007. Construction of a *Vibrio splendidus* Mutant Lacking the Metalloprotease Gene *vsm* by Use of a Novel Counterselectable Suicide Vector. Appl. Environ. Microbiol. 73, 777–784. https://doi.org/10.1128/AEM.02147-06

Leblad, B.R., Amnhir, R., Reqia, S., Sitel, F., Daoudi, M., Marhraoui, M., Abdellah, M.K.O., Veron, B., Er-Raioui, H., Laabir, M., 2020. Seasonal variations of phytoplankton assemblages in relation to environmental factors in Mediterranean coastal waters of Morocco, a focus on HABs species. Harmful Algae 96, 101819. https://doi.org/10.1016/j.hal.2020.101819

Lemire, A., Goudenege, D., Versigny, T., Petton, B., Calteau, A., Labreuche, Y., Le Roux, F., 2015. Populations, not clones, are the unit of vibrio pathogenesis in naturally infected oysters. Isme J. 9, 1523–1531. https://doi.org/10.1038/ismej.2014.233

LeRoux, F., Wegner, K.M., Baker-Austin, C., Vezzulli, L., Osorio, C.R., Amaro, C., Ritchie, J.M., Defoirdt, T., Destoumieux-Garzon, D., Blokesch, M., Mazel, D., Jacq, A., Cava, F., Gram, L., Wendling, C.C., Strauch, E., Kirschner, A., Huehn, S., 2015. The emergence of Vibrio pathogens in Europe: ecology, evolution, and pathogenesis (Paris, 11-12th March 2015). Front. Microbiol. 6, 830. https://doi.org/10.3389/fmicb.2015.00830

Li, D., Zhang, H., Fu, L., An, X., Zhang, B., Li, Y., Chen, Z., Zheng, W., Yi, L., Zheng, T., 2014. A Novel Algicide: Evidence of the Effect of a Fatty Acid Compound from the Marine Bacterium, Vibrio sp BS02 on the Harmful Dinoflagellate, Alexandrium tamarense. Plos One 9, e91201. https://doi.org/10.1371/journal.pone.0091201

Liu, P.-C., Lee, K.-K., Yii, K.-C., Kou, G.-H., Chen, S.-N., 1996. News & Notes: Isolation of Vibrio harveyi from Diseased Kuruma Prawns Penaeus japonicus. Curr. Microbiol. 33, 129–132. https://doi.org/10.1007/s002849900087

Lopez-Joven, C., Rolland, J.-L., Haffner, P., Caro, A., Roques, C., Carre, C., Travers, M.-A., Abadie, E., Laabir, M., Bonnet, D., Destoumieux-Garzon, D., 2018. Oyster Farming, Temperature, and Plankton Influence the Dynamics of Pathogenic Vibrios in the Thau Lagoon. Front. Microbiol. 9, 2530. https://doi.org/10.3389/fmicb.2018.02530

Mandel, M.J., Stabb, E.V., Ruby, E.G., 2008. Comparative genomics-based investigation of resequencing targets in Vibrio fischeri: Focus on point miscalls and artefactual expansions. Bmc Genomics 9, 138. https://doi.org/10.1186/1471-2164-9-138

Marampouti, C., Buma, A.G.J., De Boer, M.K., 2021. Mediterranean alien harmful algal blooms: origins and impacts. Environ. Sci. Pollut. Res. 28, 3837–3851. https://doi.org/10.1007/s11356-020-10383-1

Martin, J., Fitzwater, S., 1988. Iron-Deficiency Limits Phytoplankton Growth in the Northeast Pacific Subarctic. Nature 331, 341–343. https://doi.org/10.1038/331341a0

Martin, M.O., 2002. Predatory prokaryotes: An emerging research opportunity. J. Mol. Microbiol. Biotechnol. 4, 467–477.

Mavian, C., Paisie, T.K., Alam, M.T., Browne, C., Beau De Rochars, V.M., Nembrini, S., Cash, M.N., Nelson, E.J., Azarian, T., Ali, A., Morris, J.G., Salemi, M., 2020. Toxigenic Vibrio cholerae evolution and establishment of reservoirs in aquatic ecosystems. Proc. Natl. Acad. Sci. 117, 7897–7904. https://doi.org/10.1073/pnas.1918763117

McRose, D.L., Baars, O., Seyedsayamdost, M.R., Morel, F.M.M., 2018. Quorum sensing and iron regulate a two-for-one siderophore gene cluster in *Vibrio harveyi*. Proc. Natl. Acad. Sci. 115, 7581–7586. https://doi.org/10.1073/pnas.1805791115

Miethke, M., Marahiel, M.A., 2007. Siderophore-Based Iron Acquisition and Pathogen Control. Microbiol. Mol. Biol. Rev. 71, 413–451. https://doi.org/10.1128/MMBR.00012-07

Miller, S.D., Haddock, S.H.D., Elvidge, C.D., Lee, T.F., 2005. Detection of a bioluminescent milky sea from space. Proc. Natl. Acad. Sci. U. S. A. 102, 14181–14184. https://doi.org/10.1073/pnas.0507253102

Millero, F.J., 1998. Solubility of Fe(III) in seawater. Earth Planet. Sci. Lett. 154, 323–329. https://doi.org/10.1016/S0012-821X(97)00179-9

Muhling, B.A., Jacobs, J., Stock, C.A., Gaitan, C.F., Saba, V.S., 2017. Projections of the future occurrence, distribution, and seasonality of three Vibrio species in the Chesapeake Bay under a high-emission climate change scenario. Geohealth 1, 278–296. https://doi.org/10.1002/2017GH000089

Neilands, J., 1981. Iron-Absorption and Transport in Microorganisms. Annu. Rev. Nutr. 1, 27–46. https://doi.org/10.1146/annurev.nu.01.070181.000331

Oberbeckmann, S., Fuchs, B.M., Meiners, M., Wichels, A., Wiltshire, K.H., Gerdts, G., 2012. Seasonal Dynamics and Modeling of a Vibrio Community in Coastal Waters of the North Sea. Microb. Ecol. 63, 543–551. https://doi.org/10.1007/s00248-011-9990-9

Pal, M., Yesankar, P.J., Dwivedi, A., Qureshi, A., 2020. Biotic control of harmful algal blooms (HABs): A brief review. J. Environ. Manage. 268, 110687. https://doi.org/10.1016/j.jenvman.2020.110687

Papenfort, K., Bassler, B.L., 2016. Quorum sensing signal-response systems in Gram-negative bacteria. Nat. Rev. Microbiol. 14, 576–588. https://doi.org/10.1038/nrmicro.2016.89

Perez, J., Moraleda-Munoz, A., Javier Marcos-Torres, F., Munoz-Dorado, J., 2016. Bacterial predation: 75 years and counting! Environ. Microbiol. 18, 766–779. https://doi.org/10.1111/1462-2920.13171

Pfaffl, M.W., 2001. A new mathematical model for relative quantification in real-time RT-PCR. Nucleic Acids Res. 29, e45. https://doi.org/10.1093/nar/29.9.e45

Rashidan, K.K., Bird, D.F., 2001. Role of predatory bacteria in the termination of a cyanobacterial bloom. Microb. Ecol. 41, 97–105.

Rodrigues, A.M.S., Lami, R., Escoubeyrou, K., Intertaglia, L., Mazurek, C., Doberva, M., Pérez-Ferrer, P., Stien, D., 2022. Straightforward *N* -Acyl Homoserine Lactone Discovery and Annotation by LC–MS/MS-based Molecular Networking. J. Proteome Res. 21, 635–642. https://doi.org/10.1021/acs.jproteome.1c00849

Rolland, J.-L., Pelletier, K., Masseret, E., Rieuvilleneuve, F., Savar, V., Santini, A., Amzil, Z., Laabir, M., 2012. Paralytic Toxins Accumulation and Tissue Expression of alpha-Amylase and Lipase Genes in the Pacific Oyster Crassostrea gigas Fed with the Neurotoxic Dinoflagellate Alexandrium catenella. Mar. Drugs 10, 2519–2534. https://doi.org/10.3390/md10112519

Romano, A., Trimble, L., Hobusch, A.R., Schroeder, K.J., Amin, S.A., Hartnett, A.D., Barker, R.A., Crumbliss, A.L., Carrano, C.J., 2013. Regulation of iron transport related genes by boron in the marine bacterium Marinobacter algicola DG893. Metallomics 5, 1025. https://doi.org/10.1039/c3mt00068k

Rosales, D., Ellett, A., Jacobs, J., Ozbay, G., Parveen, S., Pitula, J., 2022. Investigating the Relationship between Nitrate, Total Dissolved Nitrogen, and Phosphate with Abundance of Pathogenic Vibrios and Harmful Algal Blooms in Rehoboth Bay, Delaware. Appl. Environ. Microbiol. 88, e00356-22. https://doi.org/10.1128/aem.00356-22

Sinclair, A.R.E., Mduma, S., Brashares, J.S., 2003. Patterns of predation in a diverse predator-prey system. Nature 425, 288–290. https://doi.org/10.1038/nature01934

Su, R.Q., Yang, X.R., Zheng, T.L., Tian, Y., Jiao, N.Z., Cai, L.Z., Hong, H.S., 2007. Isolation and characterization of a marine algicidal bacterium against the toxic dinoflagellate Alexandrium tamarense. Harmful Algae 6, 799–810. https://doi.org/10.1016/j.hal.2007.04.004

Tanabe, T., Funahashi, T., Nakao, H., Miyoshi, S.-I., Shinoda, S., Yamamoto, S., 2003. Identification and Characterization of Genes Required for Biosynthesis and Transport of the Siderophore Vibrioferrin in *Vibrio parahaemolyticus*. J. Bacteriol. 185, 6938–6949. https://doi.org/10.1128/JB.185.23.6938-6949.2003

Thompson, F.L., Thompson, C.C., Swings, J., 2003. Vibrio tasmaniensis sp. nov., isolated from Atlantic Salmon (Salmo salar L.). Syst. Appl. Microbiol. 26, 65–69. https://doi.org/10.1078/072320203322337326

Tourneroche, A., Lami, R., Hubas, C., Blanchet, E., Vallet, M., Escoubeyrou, K., Paris, A., Prado, S., 2019. Bacterial–Fungal Interactions in the Kelp Endomicrobiota Drive Autoinducer-2 Quorum Sensing. Front. Microbiol. 10, 1693. https://doi.org/10.3389/fmicb.2019.01693

Vanhove, A.S., Rubio, T.P., Nguyen, A.N., Lemire, A., Roche, D., Nicod, J., Vergnes, A., Poirier, A.C., Disconzi, E., Bachere, E., Le Roux, F., Jacq, A., Charriere, G.M., Destoumieux-Garzon, D., 2016. Copper homeostasis at the host vibrio interface: lessons from intracellular vibrio transcriptomics. Environ. Microbiol. 18, 875–888. https://doi.org/10.1111/1462-2920.13083

Wang, X., Li, Z., Su, J., Tian, Y., Ning, X., Hong, H., Zheng, T., 2010. Lysis of a red-tide causing alga, Alexandrium tamarense, caused by bacteria from its phycosphere. Biol. Control 52, 123–130. https://doi.org/10.1016/j.biocontrol.2009.10.004

Wang, Y., Li, S., Liu, G., Li, X., Yang, Q., Xu, Y., Hu, Z., Chen, C.-Y., Chang, J.-S., 2020. Continuous production of algicidal compounds against Akashiwo sanguinea via a Vibrio sp. co-culture. Bioresour. Technol. 295, 122246. https://doi.org/10.1016/j.biortech.2019.122246

Weerasinghe, A.J., Amin, S.A., Barker, R.A., Othman, T., Romano, A.N., Parker Siburt, C.J., Tisnado, J., Lambert, L.A., Huxford, T., Carrano, C.J., Crumbliss, A.L., 2013. Borate as a Synergistic Anion for *Marinobacter algicola* Ferric Binding Protein, FbpA: A Role for Boron in Iron Transport in Marine Life. J. Am. Chem. Soc. 135, 14504–14507. https://doi.org/10.1021/ja406609s

Wu, J., Luther, G., 1994. Size-Fractionated Iron Concentrations in the Water Column of the Western North-Atlantic Ocean. Limnol. Oceanogr. 39, 1119–1129. https://doi.org/10.4319/lo.1994.39.5.1119

Xu, Q., Wang, P., Huangleng, J., Su, H., Chen, P., Chen, X., Zhao, H., Kang, Z., Tang, J., Jiang, G., Li, Z., Zou, S., Dong, K., Huang, Y., Li, N., 2022. Co-occurrence of chromophytic phytoplankton and the Vibrio community during Phaeocystis globosa blooms in the Beibu Gulf. Sci. Total Environ. 805, 150303. https://doi.org/10.1016/j.scitotenv.2021.150303

Yang, Q., Feng, Q., Zhang, B., Gao, J., Sheng, Z., Xue, Q., Zhang, X., 2021. Marinobacter alexandrii sp. nov., a novel yellow-pigmented and algae growth-promoting bacterium isolated from marine phycosphere microbiota. Antonie Van Leeuwenhoek Int. J. Gen. Mol. Microbiol. 114, 709–718. https://doi.org/10.1007/s10482-021-01551-5

784 Zhang, W., Wang, Y., Lu, H., Liu, Q., Wang, C., Hu, W., Zhao, K., 2020. Dynamics of Solitary Predation by
785 Myxococcus xanthus on Escherichia coli Observed at the Single-Cell Level. Appl. Environ.
786 Microbiol. 86, e02286-19. https://doi.org/10.1128/AEM.02286-19
787

ACKNOWLEDGMENT

The authors thank F. Le Roux and Y. Labreuche for their gift of *Vibrio* mutants; E. Garcés, S. Turki, H. Frehi, A. Bouquet and W. Medhioub for their contribution in obtaining Mediterranean phytoplankton strains; K. Escoubeyrou and D. Stien for advice on HRMS/MS data; V. Diakou-Verdin and E. Jublanc from the Montpellier RIO Imaging Platform for access to microscope facilities (www.mri.cnrs.fr); P. Clair from the Montpellier qPHD platform and the Technoviv platform of the UPVD for access to PCR facilities; Luc Markiw, N. Brunet, A. Lang, A. Payelleville, T. Milhau and M. Leroy for their technical assistance; The IFREMER LER-LR laboratory for access to the Thau Lagoon; the BIO2MAR platform at the Observatoire Océanologique de Banyuls for providing access to UHPLC-HRMS/MS facilities.

FUNDING

European VIVALDI grant 678589, French EC2CO ROSEOCOM grant and IFREMER ALGOVIR grant.

FIGURES, TABLES and VIDEOS

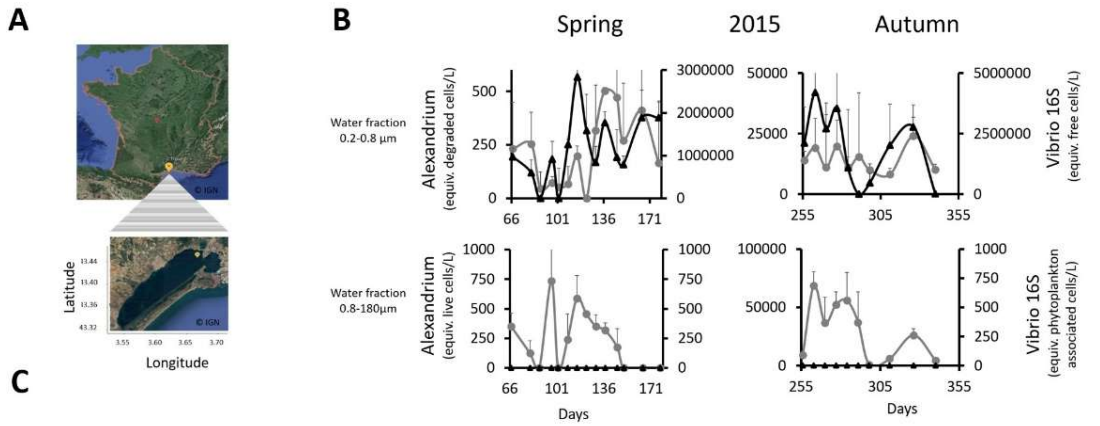

C

Model degraded Alexandrium cells	AICc
Intercept+ free Vibrio	171.77
intercept	172.57
Intercept + salinity	173.41
Intercept + temperature	173.94
Intercept+ free Vibrio + salinity	174.99
Intercept+ free Vibrio + temperature	175.37
Intercept + temperature + salinity	177.72
Intercept+ free Vibrio + temperature + salinity	180.56

D

	Estimate	Std error	T value	Pr(>|t|)
Intercept	235.41	38.69	6.08	7.91×10^{-05}
Vibrio	83.19	40.27	2.07	0.06

Figure 1. Dynamics of *Alexandrium* and *Vibrio* in the environment. (A) Location of the monitoring station in the Thau Lagoon (southern France). **(B)** Mean abundance (DNA equiv.) of *Vibrio spp*. (16S) and Alexandrium *spp*. *(A. pacificum* ACT03 + *A. tamarense* ATT07). *Vibrio* cells (black line with diamond dot) and degraded *Alexandrium* cells (grey line with round dot) were evidence in the 0.2–0.8 µm fraction (free *Vibrio* fraction) in spring and autumn 2015. Living *Alexandrium* cells (grey line with roundot) but no plankton-associated *Vibrio spp*. (black line with diamond dot) were evidence in the 0.8–180 µm in spring and autumn. **(C)** Result of Akaike information criterion (AICc) models tested to explain the mean value of degraded Alexandrium cells (dead cells) in spring. **(D)** Wald test of the AICc model attributing the mean value of degraded cells of Alexandrium in spring to free *Vibrio*.

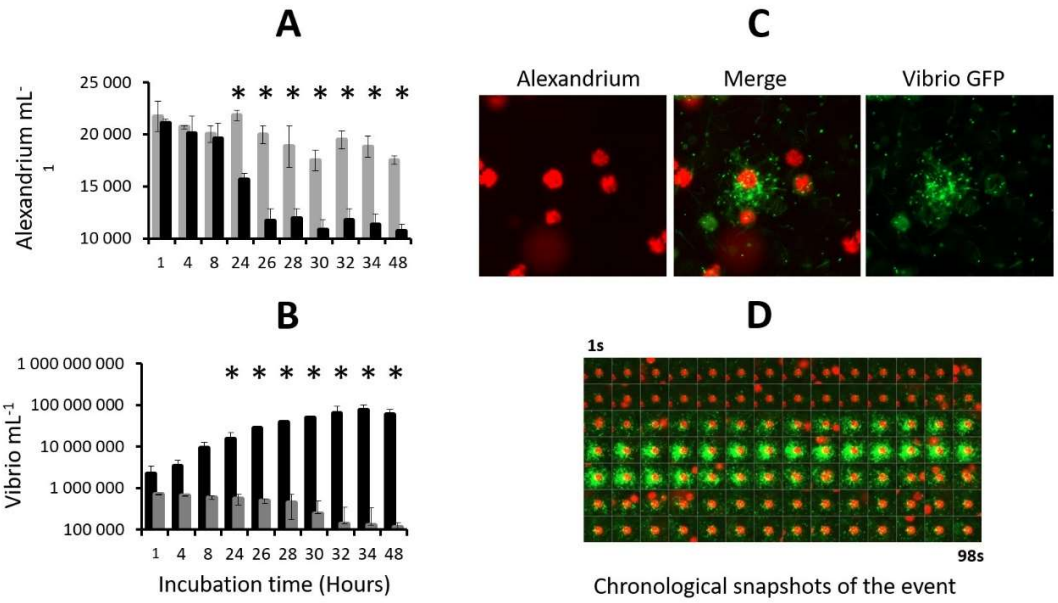

Figure 2. Incubation of *Vibrio atlanticus* LGP32 and *Alexandrium pacificum* ACT03 in enriched natural seawater (ENSW). **(A)** *A. pacificum* ACT03 cultured alone (grey bar) and incubated with *V. atlanticus* LGP32 (black bar) in ENSW. **(B)** *V. atlanticus* LGP32 cultured alone (grey bar) and incubated with *A. pacificum* ACT03 (black bar) in ENSW.**(C)** Snapshot of the interaction between *V. atlanticus* LGP32-GFP cells (60-hour culture) and one cell of *A. pacificum* ACT03 taken at 8h00 of co-culture. **(D)** Chronological snapshots of the interaction (98 pictures, one per second). *V. atlanticus* LGP32 (small green cells) and *A. pacificum* ACT03 cell (large red cell). All experiments were done in triplicates. Asterisks indicate significant differences in a multiple comparison test (One-way ANOVA with post hoc Tukey test), *$P \leq 0.05$.

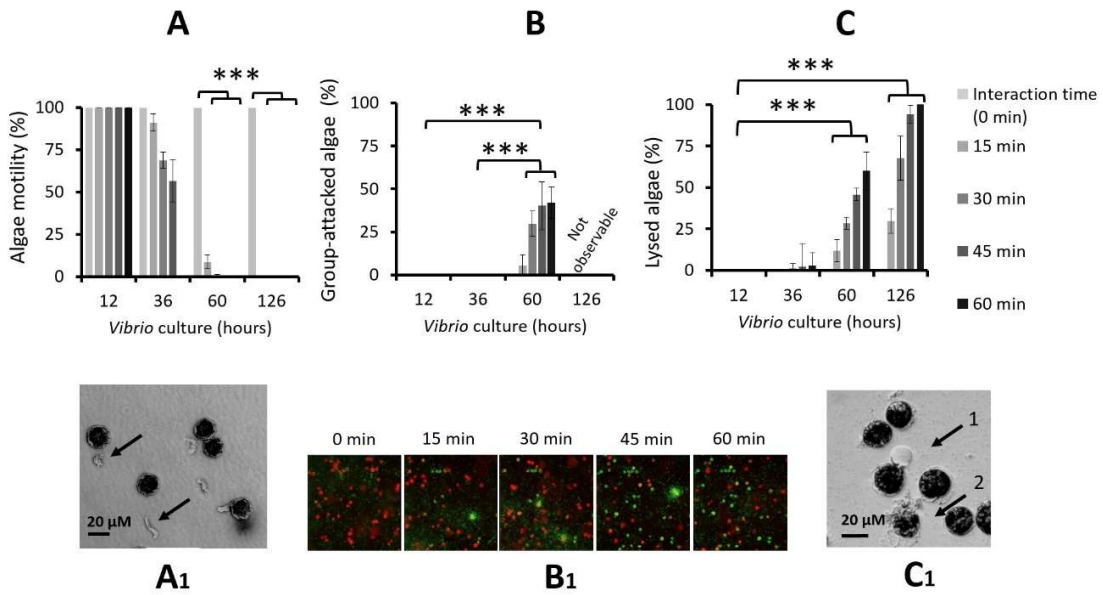

Figure 3. Role of *Vibrio atlanticus* LGP32 starvation in the interspecific interaction process. Experiments were conducted by incubating*A. pacificum* ACT03 with *V. atlanticus* LGP32 previously grown for 12, 36, 60 and 126 h in Zobell medium. **(A)** Cumulative percentage of motile *A. pacificum* ACT03 cells. **(B)** Cumulative number of cells attacked by *V. atlanticus* LGP32 and **(C**) Cumulative cell lysis after 0, 15, 30, 45 and 60 minutes of interaction. Corresponding pictures showing **(A1)** Black arrows indicate unhooked and degrade flagellum from *A. pacificum* ACT03 flagellum, **(B1)** Chronological sequence of five snapshots showing *V. atlanticus* LGP32-GFP cells (60-hour culture) and *A. pacificum* ACT03 cells, during the first hour of their interaction. *V. atlanticus* LGP32 (small green cells), living *A. pacificum* ACT03 (large red cells) and dead *A. pacificum* ACT03 (large green cell). **(C1)** Black arrow 1 indicate vesicle formation on *A. pacificum* ACT03 cell and black arrow 2 indicate lysed *A. pacificum* ACT03 cell. All percentages were determined based on a minimum of 2,000 cells of *A. pacificum* ACT03. All experiments were done in triplicates. Asterisks indicate significant differences in a multiple comparison test (One-way ANOVA with post hoc Tukey test), ***$P \leq 0.001$

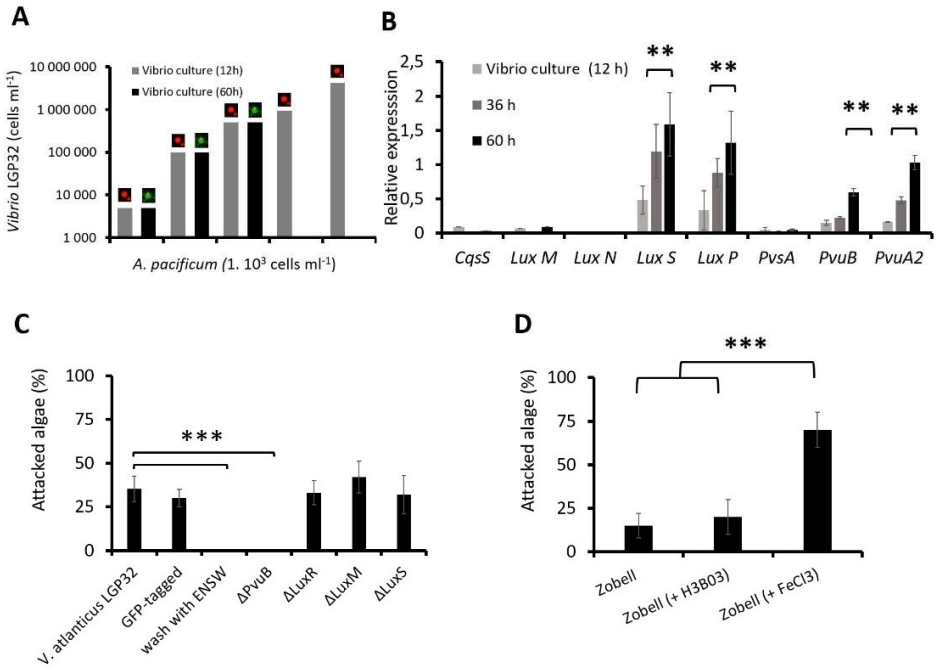

Figure 4. Role of quorum sensing and the vibrioferrin iron uptake pathway in the interaction process. **(A)** Effect of *V. atlanticus* LGP32 cell density on the attack process. *A. pacificum* ACT03 cells (1.10^3 cells mL^{-1}) were incubated with *V. atlanticus* LGP32 grown for 60 hours in Zobell medium at concentrations ranging from 5.10^3 to 5.10^5 cells mL^{-1} (black bars). For comparison, *A. pacificum* ACT03 incubated with *V. atlanticus* LGP32 grown for 12 hours in Zobell medium at concentrations ranging from 5.10^3 to 4.10^6 cells mL−1 (grey bars). The image on the bars indicates either unaffected algae (live red algae) or algae attacked by vibrio's (algae covered with green vibrio's) during the interaction **(B)** CqsS, luxM, luxN, luxS, and luxP quorum sensing and PvsA, PvuB and PvuA2 vibrioferrin pathway genes expression in *V. atlanticus* LGP32 grown for 12, 36 and 60 h in Zobell medium. **(C)** Effect of *V. atlanticus* LGP32 mutants on the attacked process. Experiments were conducted by incubating *A. pacificum* ACT03 with *V. atlanticus* LGP32, *V. atlanticus* LGP32 tagged with GFP, *V. atlanticus* LGP32 washed with ENSW or *V. atlanticus* LGP32 mutant ΔPvuB, ΔluxM, ΔluxR and ΔluxS previously grown 60 h in Zobell media (control), The percentage of *A. pacificum* ACT03 attacked was determined during the first 30 min of exposure. **(D)** Effect of *V. atlanticus* LGP32 cultures media composition on the attacked process. Experiments were conducted by incubating *A. pacificum* ACT03 with *V. atlanticus* LGP32 grown 60 h in Zobell media supplemented with H_3BO_4 or $FeCl_3$. The results were compared with an exposure to *V. atlanticus* LGP32 grown 60 h in Zobell media. All percentages were determined based on a minimum of 2,000 cells of *A. pacificum* ACT03. All experiments were done in triplicates. Asterisks indicate significant differences in a multiple comparison test (One-way ANOVA with post hoc Tukey

856 test), **P ≤ 0.01, ***P ≤ 0.001

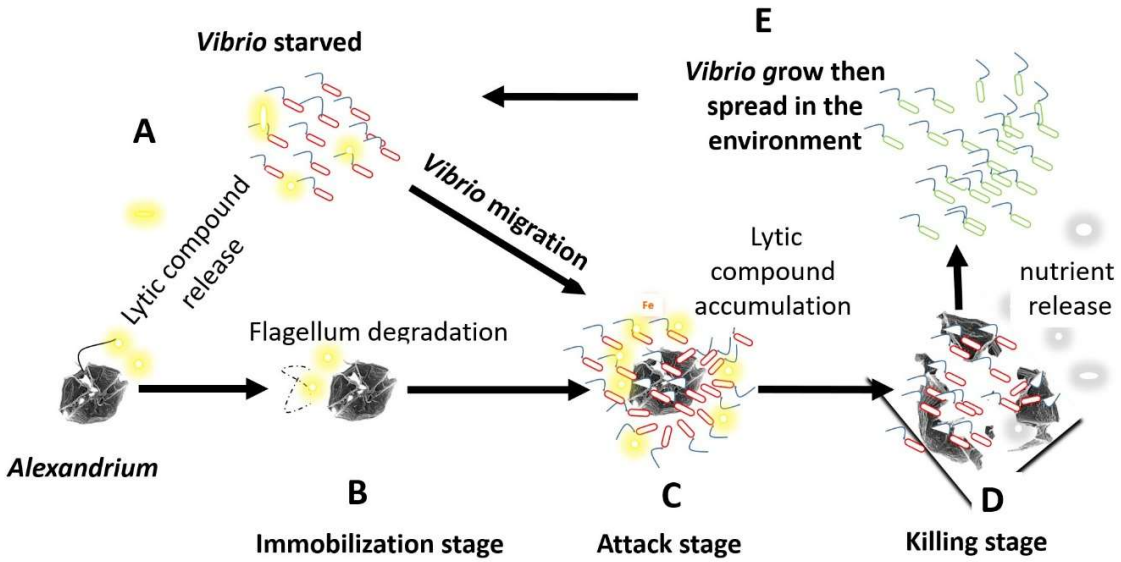

857

858 **Figure 5. Schematic representation of a putative strategy developed by *Vibrio spp*. to feed on**
859 **Alexandrium *spp*. and *G. catenatum* in the environment. (A)** *Vibrio* in the environment when subjected
860 to starvation secrete non-protein lytic compounds. **(B)** Some of these lytic compounds degrade the
861 flagella, immobilizing the alga (immobilization stage). **(C)** Then *Vibrio* swims and clusters around its prey
862 (attack stage). **(D)** Lytic compounds released by *Vibrio* where able to concentrate around the algae cells,
863 thereby lysing the algae (killing stage). **(E)** Feeding on the released nutrients, *Vibrio* multiply and then
864 spread in the environment. Yellow clouds: Lytic compound release by *Vibrio,* Grey clouds: Algal
865 nutrients released upon lysis.

866

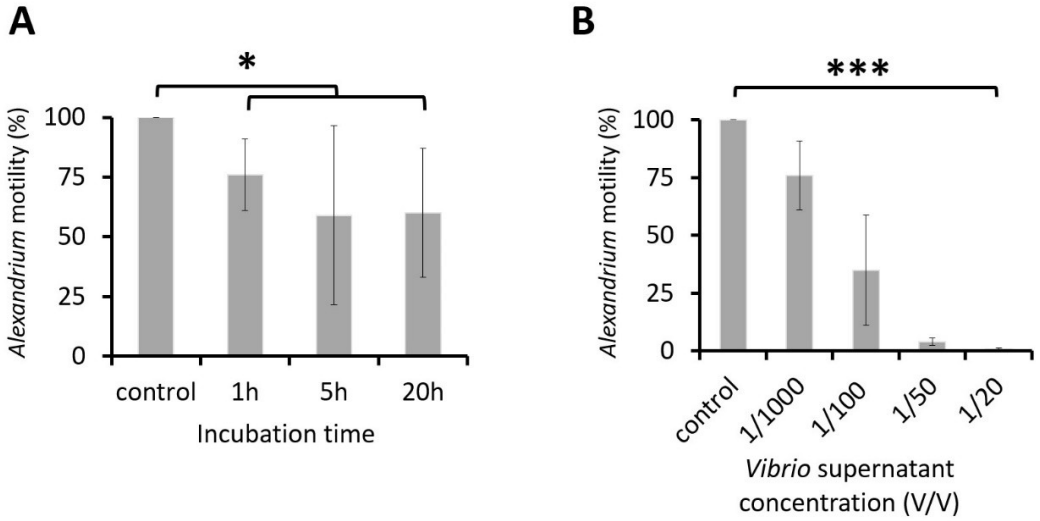

867

868 **Figure S1. Time and dose-dependent effects of the *V. atlanticus* LGP32 culture supernatant on *A.***
869 ***pacificum* ACT03 motility. (A)** A time dependence experiment was conducted by incubating *A. pacificum*
870 ACT03 for 1, 5 or 20 h with 1/1000 v/v (1 µL/mL) of culture supernatant from *V. atlanticus* LGP32
871 previously grown for 60 h in Zobell culture media. **(B)** A dose dependence experiment was conducted by
872 incubating *A. pacificum* ACT03 for 1 h with 1/1000 to 1/20 v/v (1-50 µL/mL) of culture supernatant from
873 *V. atlanticus* previously grown for 60 h in Zobell media. The percentage of motile *A. pacificum* ACT03 was
874 determined after 1 hours of exposure. All percentages were determined based on a minimum of 2,000 cells
875 of *A. pacificum* ACT03. Error bars represent the standard deviation of the mean of three independent
876 experiments. Asterisks indicate significant differences in a multiple comparison test (One-way ANOVA
877 with post hoc Tukey test), *$P \leq 0.05$, ***$P \leq 0.001$.

878

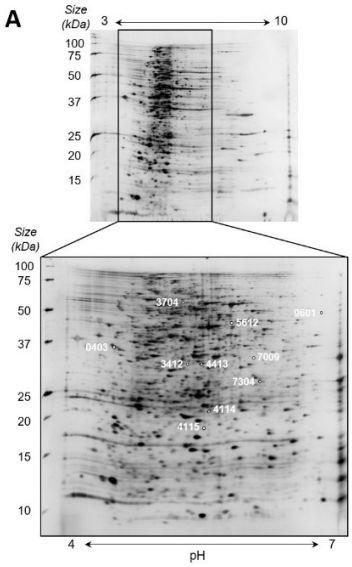

B

Spot #	Value ENSW	Value Zobell	Ratio (ENSW/Zobell)	Best ID Accession	#Peptides	-10logP Prot	-10logP Pept. Min	-10logP Pept. Max	Seq coverage	CDD accession	Best ID Description	Expected mass	Expected pI
7304	3620,4	570,7	6,34	WP_012601215.1	3	172,83	67,81	92,01	14%	PRK00443	glucosamine-6-phosphate deaminase	29610	5,53
4115	1203,8	191,9	6,27	ND									
0403	3697,4	750,2	4,93	WP_004733797.1	16	253,95	23,25	124,97	33%	cd13641	ABC transporter substrate-binding protein	36195	4,52
4413	**640,2**	**267,4**	**2,39**	**WP_012600975.1**	**21**	**241,28**	**25,81**	**101,45**	**51%**	**PRK11411**	**iron siderophore-binding protein, PvuB**	**36111**	**5,73**
7009	616,6	316,3	1,95	ND									
3704	683,2	1303	-1,91	WP_009848030.1	30	360,8	29,21	121,35	54%	PRK09344	phosphoenolpyruvate carboxykinase (ATP)	59755	4,85
4114	315,2	812,6	-2,58	WP_009847387.1	2	58,71	58,71	58,71	8%	PRK00129	uracil phosphoribosyltransferase	22658	5,21
3412	57,7	238,2	-4,13	WP_012604509.1	10	244,21	29,11	105,11	38%	cd13674	C4-dicarboxylate ABC transporter	36946	5,26
5612	211,4	1395,9	-6,60	WP_012600249.1	2	79,11	40,49	40,83	6%	PRK05451	dihydroorotase	37599	5,36
9601	76,9	1717,1	-22,33	WP_004736554.1	12	208,83	33,74	100,38	29%	PRK08722	beta-ketoacyl-{acyl-carrier-protein }synthase II	43007	5,95

879

880 **Figure S2.** ***Vibrio atlanticus*** **LGP32 proteome analysis following nutrient stress. (A)** Example of 2D
881 gel, the numbers in white on the gel 4-7 correspond to the number and position of the protein spots
882 analyzed. **(B)** Proteins identified by LC-MS/MS as differentially represented in the 2D gel comparative
883 approach following nutrient stress. ND: Not determined; ENSW (artificial seawater)**.**

884

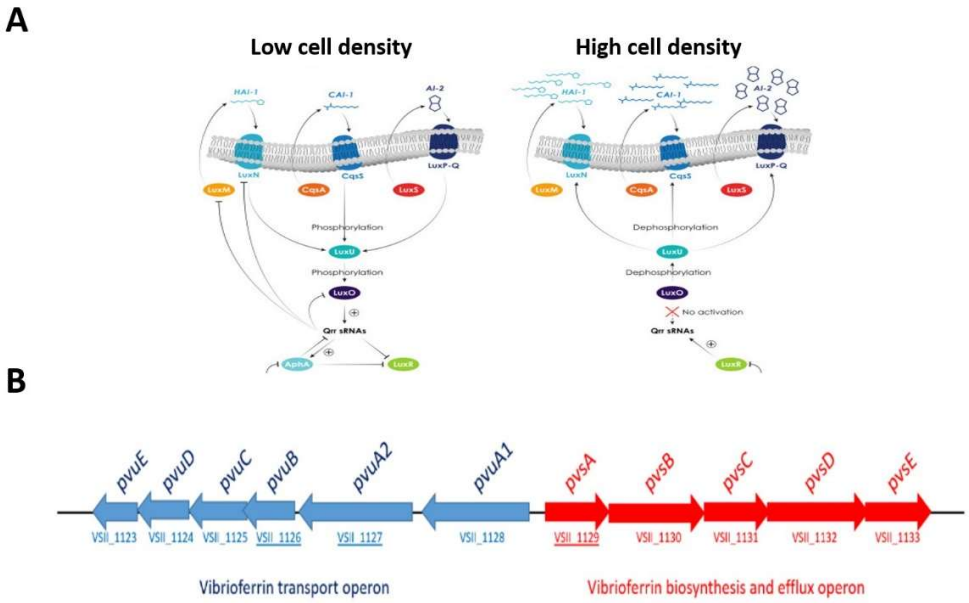

885

886 **Figure S3. Quorum sensing and the vibrioferrin iron uptake pathway in *Vibrio*. (A)** Putative quorum
887 sensing (QS) pathways at low and high cell density in *Vibrio* according to Lami et al.(Lami, 2019). **(B)**
888 Genetic organization of the vibrioferrin utilization gene cluster on *V. atlanticus* LGP32 chromosome 2.
889 The Pvu and Pvs operons are involved in the secretion and the transport of ferric vibrioferrin and
890 biosynthesis of vibrioferrin, respectively. Arrows indicate the transcriptional directions of the genes.
891 VSII1126, VSII1137 and VSII1129 corresponding to PvuB, PvuA2 and PvsA genes respectively.

892 **Table 1.** Ability of Vibrio strains to attack and to lyse *Alexandrium pacificum*. ND: not determined.

Vibrio species	Strains	Virulence for fish or invertebrates	References	Attack *A. pacificum*	Lyse *A. pacificum*
Vibrio atlanticus LGP32	WT	Yes	(Gay et al., 2004)	+	+
//	WT + pSW3654T-GFP	Yes	(Le Roux et al., 2007)	+	+
//	ΔLuxM	ND	Ifremer Institute, France	+	+
//	ΔLuxS	ND	//	+	+
//	ΔLuxR	ND	//	+	+
//	ΔPvuB	ND	This work	-	+
Vibrio tasmaniensis	J5-9	Yes	(Lemire et al., 2015)	+	+
//	LMG20012^{T}	No	(Thompson et al., 2003)	+	+
Vibrio crassostreae	J2.9	Yes	(Lemire et al., 2015)	+	+
//	J2-8	No	//	+	+
Vibrio fischeri	ES114	ND	(Mandel et al., 2008)	+	+
Vibrio harveyi	ATCC14126	Yes	(Liu et al., 1996)	+	+
Vibrio aestuarianus	janv-32	Yes	(Labreuche et al., 2010)	+	+

893

894 **Table 2.** Ability of *Vibrio Atlanticus* LGP32 to degrade flagella, attack and lyse the targeted
895 dinoflagellates *spp*. commonly found in the Mediterranean Sea. ND not determined.

Dinoflagellates species	Strains	Toxicity for human	References	Flagella degraded	Cells Attacked	Cells Lysed
Alexandrium pacificum	ACT03, Thau, France	Yes	(Laabir et al., 2011)	+	+	+
Alexandrium catenella	Bizerte, Tunisia	Yes	(Fertouna-Bellakhal et al., 2015)	+	+	+
//	F3-9F, Tarragona, Spain	ND	//	+	+	+
//	C10-5, Annaba, Algeria	Yes	(Hadjadji et al., 2020)	+	+	+
Alexandrium tamarense	ATT07, Thau, France	No	(Rolland et al., 2012)	+	+	+
Alexandrium spp.	Golf of Tunis, Tunisia	ND	Algal collection university of Montpellier, France	+	+	+
//	Bizerte, Tunisia	ND	//	+	+	+
//	Mediterranean coast, Morocco	ND	//	+	+	+
Prorocentrum lima	PLBZT14, Bizerte, Tunisia	Yes	(Ben-Gharbia et al., 2016)	-	-	-
Coolia monotis	CMBZT14, Bizerte, Tunisia	ND	//	-	-	-
Vulcanodinium rugosum	IFR-VRU-01, Ingril, France	Yes	(Abadie et al., 2015)	-	-	-
Karenia selliformis	Golf of Gabes, Tunisia	ND	Algal collection university of Montpellier, France	-	-	-
Scripsiella trochoidae	Mellah Lagoon, Algeria	-	//	-	-	-
Gyrodinium impudicum	Golf of Tunis, Tunisia	-	//	-	-	-
Amphidium carterae	SAMS, Scotland	ND	SAMS laboratory, Scotland	-	-	-
Gymnodinium catenatum	M'diq Bay, Morocco	+	(Leblad et al., 2020)	+	+	+

896

897 **Table 3.** Oligonucleotide sequences of primers used for RNA expression analysis.

Species	genes	Primers Sequences	Tm (°C)	Efficiency	References
Alexandrium pacificum (ACT03)	18S – 28S rRNA ITS region	TGATATTGTGGGCAACTGTAA AACATCTGTTAGCTCACGGAA	54		(Genovesi et al., 2011)
Alexandrium tamarense (ATT07)	18S – 28S rRNA ITS region	TGGTAATTCTTCATTGATTACAATG AACATCTGTTAGCTCACGGAA	54		//
Vibrios spp.	16S	CGGTGAAATGCGTAGAGAT TTACTAGCGATTCCGAGTTC	62		(Kitatsukamoto et al., 1993)
Vibrio atlanticus LGP32	LuxN (VS_II0260)	CACTTGCTAGTATCATCGC ATCGAGTTAGCAAGAGCAC	60	1,92	This work
//	LuxM (VS_II0261)	TCCACTTATCACAAACAGG ACTGTACTTCCATTTGTCG	60	1,91	//
//	LuxP (VS_II0355)	AAGTTCAGGATGAACCTATC CAAAGAGATACTTTGCTGAG	60	1,89	//
//	LuxS (VS_2562)	ACTCTCGAGCACCTATACG GAAGGCGTACCAATCAAGC	60	1,85	//
//	CqsS (VS_1725)	GACATCTATTGATGTTATGC TCACCCACTTCACGTAACTG	60	1,91	//
//	PvsA (VS_II0355),Vibrioferrin biosynthesis protein	CAGAGCAAGAGCTAGAACC TCGTTGAGAACCTGACGAG	59	1,91	//
//	PvuB (VS_II1126), ABC transporter vibrioferrin uptake FecB	TAGTGCAACCATGGGAATCG TAAACCGTACGTAGACGCTC	57	2,01	//
//	PvuA2 (VS_II1127), Vibrioferrin receptor FecA	GGAGCTACAAGCATTCGTTC TTCGTCATATGGTCGCTTCG	57	2,08	//
//	Housekiping gene 1, CcmC (VS_0852)	ATTGCCGCCTTTATCGGTTT CAAGCACCCCACATTGGTTT	60		(Vanhove et al., 2016)
//	Housekiping gene 2, 6-phosphofructokinase (VS_2913)	GCCGTCACTGTGGTGACCTT TGCTTCTTGCCTTTCGCAAT	60		//

898

VIDEOS

Video 1. Dynamics of *Vibrio atlanticus* LGP32-*Alexandrium pacificum* ACT03 interaction. GFP-tagged *V. atlanticus* (small green cells); living *A. pacificum* (large red cells); lysed *A. pacificum* (large green cells) filmed under an epifluorescence microscope.

Video 2. Second-by-second timing of *Vibrio Atlanticus* LGP32 attacking *Alexandrium pacificum* ACT03. GFP-tagged *V. atlanticus* (small green cells); *A. pacificum* living cell (large red cells) filmed under an epifluorescence microscope**.**

Video 3. Degradation and disruption of *Alexandrium pacificum* ACT03 flagella. Effect of *Vibrio* supernatant on the first stage of the interaction filmed under a confocal microscope.

Video 4. Attacks of *Vibrio atlanticus* LGP32 on target *Alexandrium pacificum* ACT03. This video, recorded under a confocal microscope, shows Vibrios simultaneously attacking a first immobilized Alexandrium cell, then moving on to attack a second cell without ever targeting the other cells present, suggesting active communication between the Vibrio bacteria. *V. atlanticus* LGP32 (small cells); *A. pacificum* ACT03 (large cells).

Video 5. Vesicle formation and bursting of an *Alexandrium pacificum* ACT03. Direct effect of *Vibrio* supernatant on *Alexandrium* after 126 h of culture filmed under a confocal microscope.

A

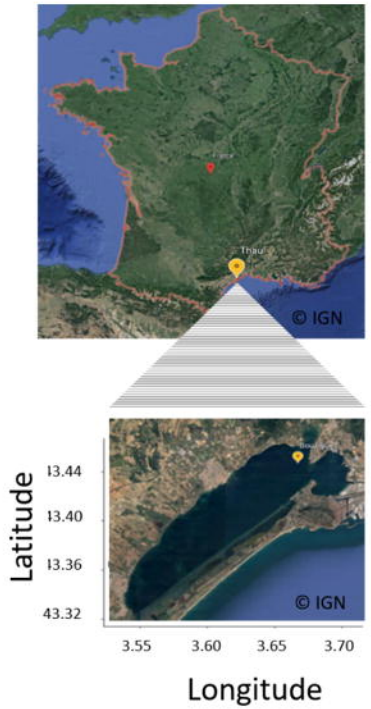

B

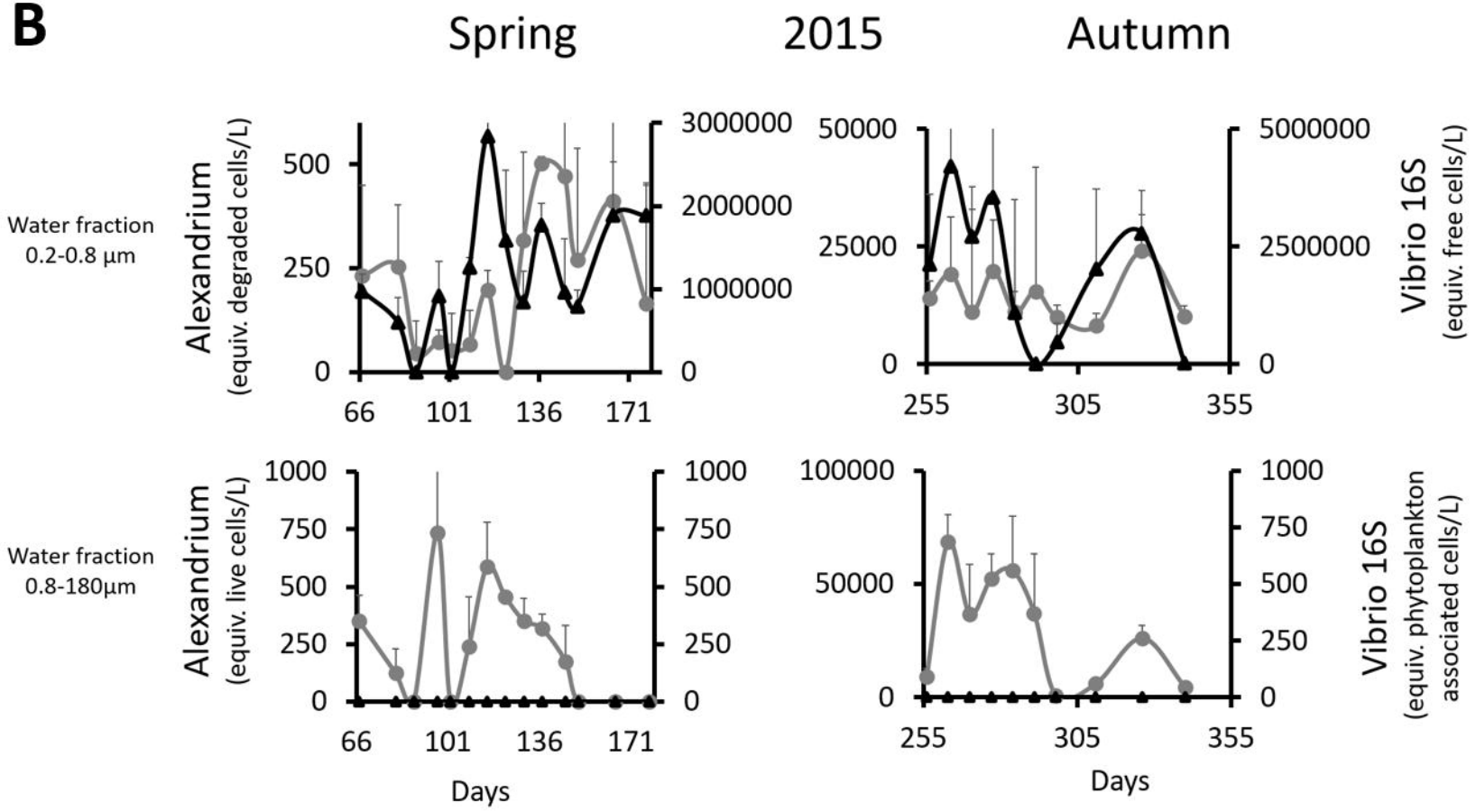

C

Model degraded Alexandrium cells	AICc
Intercept+ free Vibrio	171.77
intercept	172.57
Intercept + salinity	173.41
Intercept + temperature	173.94
Intercept+ free Vibrio + salinity	174.99
Intercept+ free Vibrio + temperature	175.37
Intercept + temperature + salinity	177.72
Intercept+ free Vibrio + temperature + salinity	180.56

D

	Estimate	Std error	T value	Pr(>|t|)
Intercept	235.41	38.69	6.08	7.91×10^{-05}
Vibrio	83.19	40.27	2.07	0.06

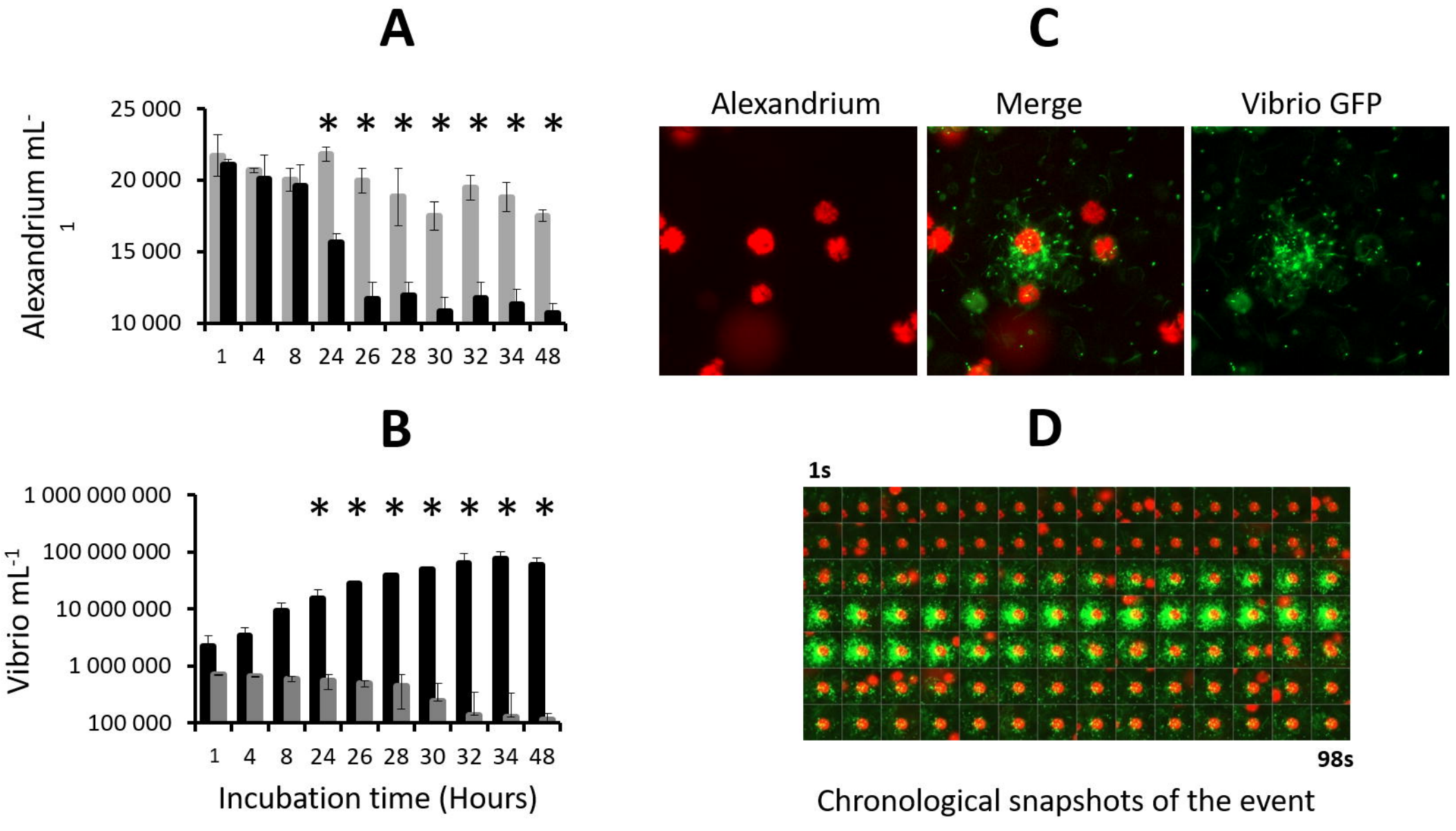
A
Alexandrium mL-1
25 000
20 000
15 000
10 000
* * * * * * *
1 4 8 24 26 28 30 32 34 48
B
Vibrio mL-1
1 000 000 000
100 000 000
10 000 000
1 000 000
100 000
* * * * * * *
1 4 8 24 26 28 30 32 34 48
Incubation time (Hours)
C
Alexandrium
Merge
Vibrio GFP
D
1s
98s
Chronological snapshots of the event

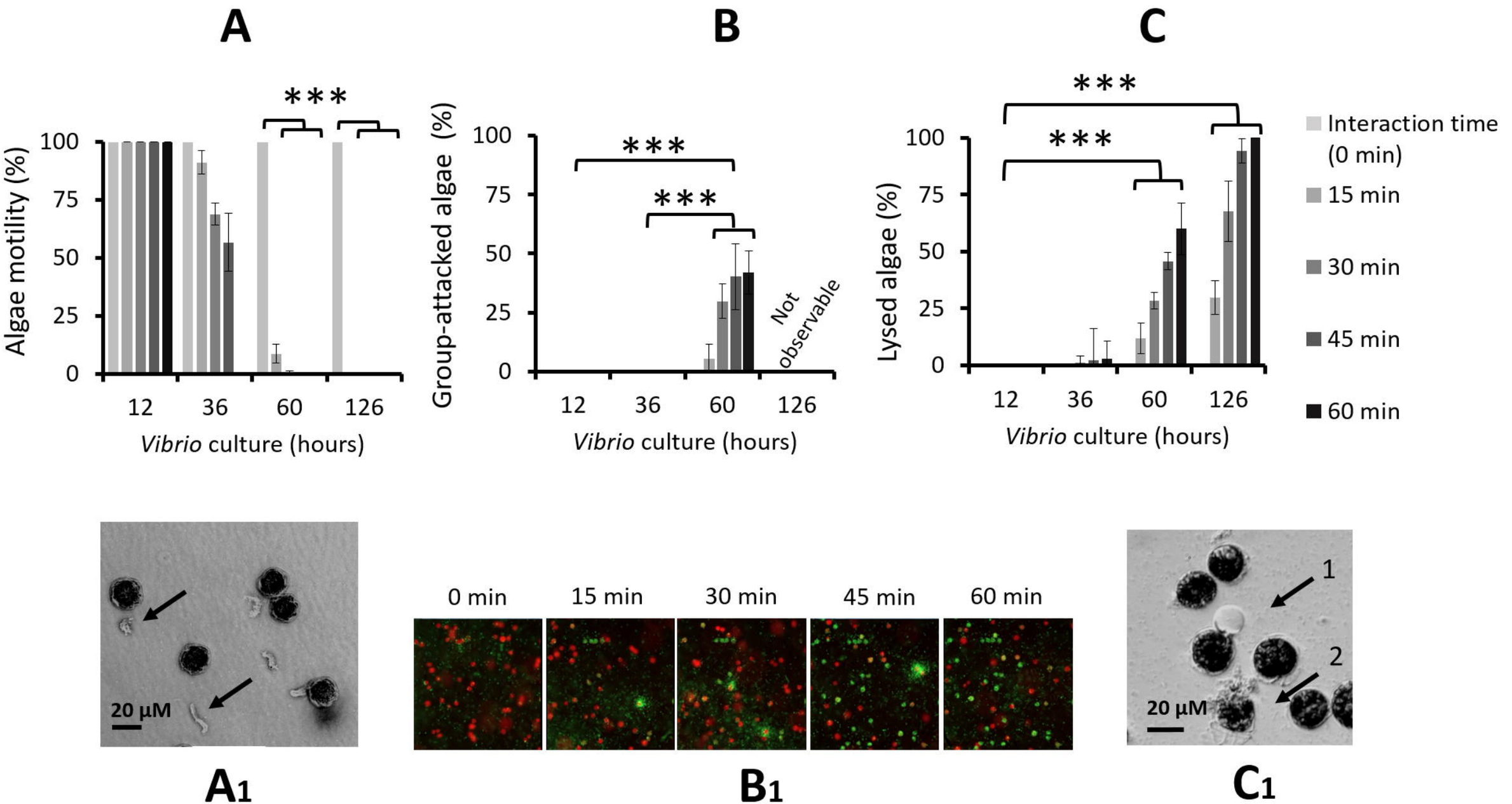
A
B
C
***
Algae motility (%)
100
75
50
25
0
12
36
60
126
Vibrio culture (hours)
Group-attacked algae (%)
Not observable
Lysed algae (%)
Interaction time (0 min)
15 min
30 min
45 min
60 min
20 µM
0 min
15 min
30 min
45 min
60 min
1
2
A1
B1
C1

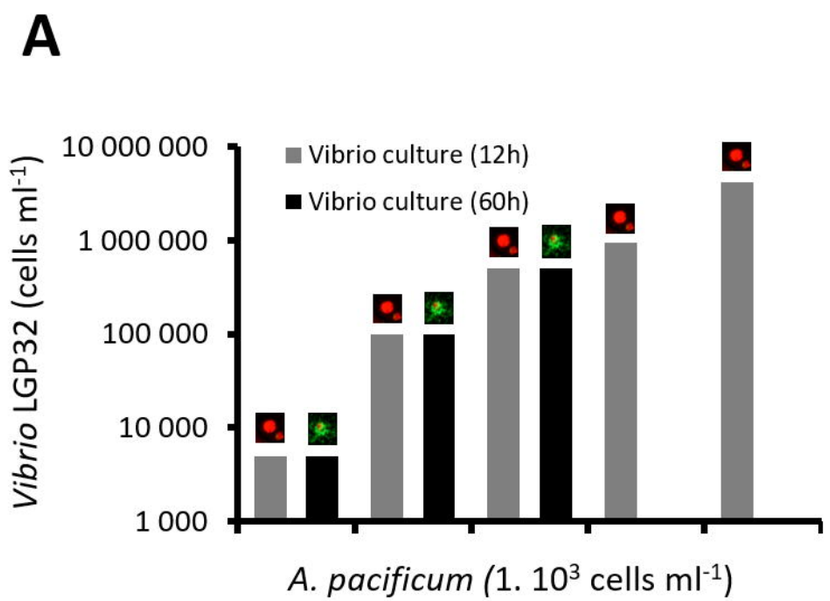
A
Vibrio culture (12h)
Vibrio culture (60h)
10 000 000
1 000 000
100 000
10 000
1 000
Vibrio LGP32 (cells ml-1)
A. pacificum (1. 10³ cells ml-1)

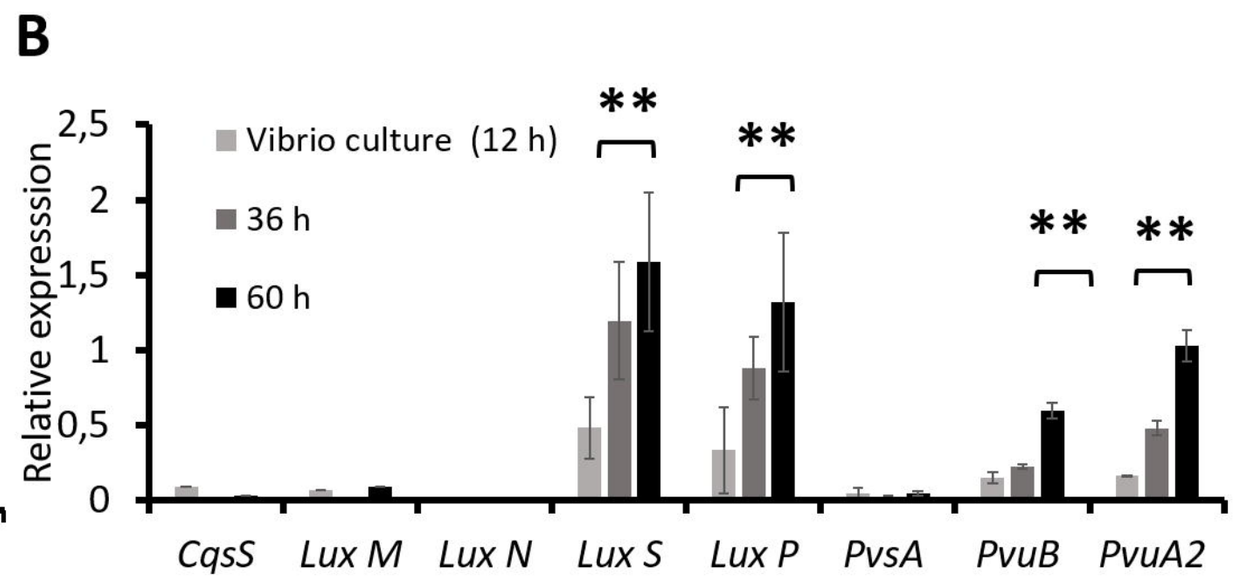
B
Vibrio culture (12 h)
36 h
60 h
Relative expresssion
2,5
2
1,5
1
0,5
0
**
**
**
**
CqsS
Lux M
Lux N
Lux S
Lux P
PvsA
PvuB
PvuA2

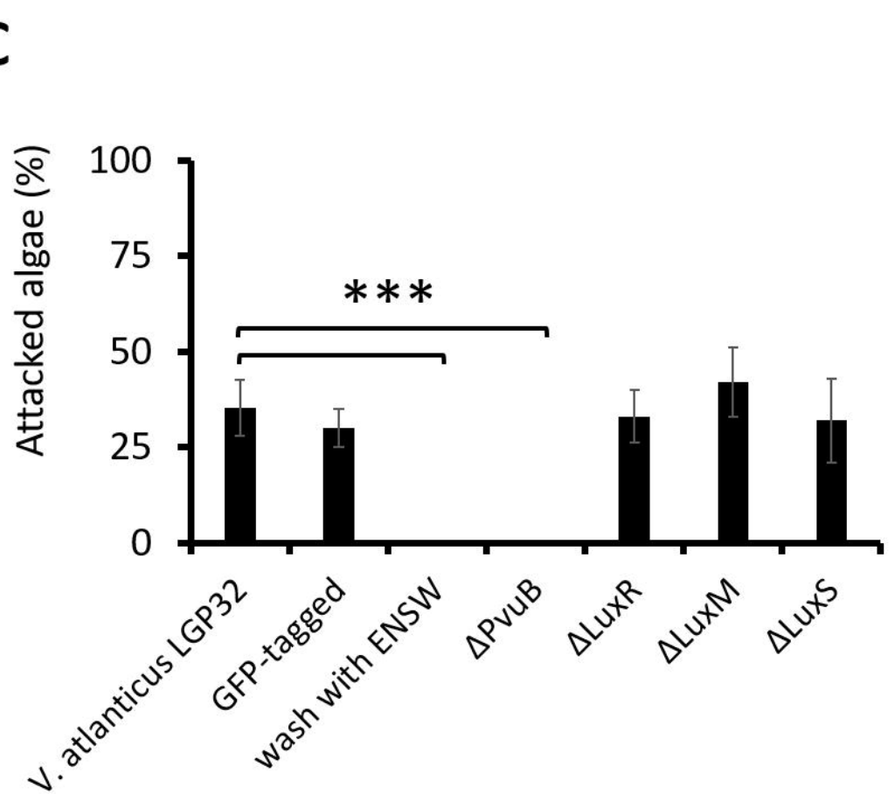
C
Attacked algae (%)
100
75
50
25
0
***
V. atlanticus LGP32
GFP-tagged
wash with ENSW
ΔPvuB
ΔLuxR
ΔLuxM
ΔLuxS

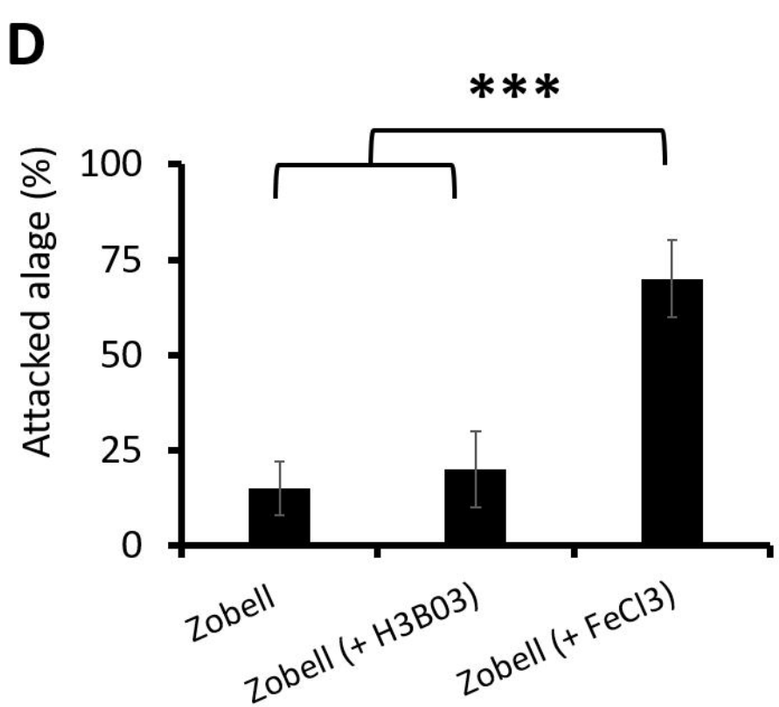
D
***
Attacked alage (%)
100
75
50
25
0
Zobell
Zobell (+ H3B03)
Zobell (+ FeCl3)

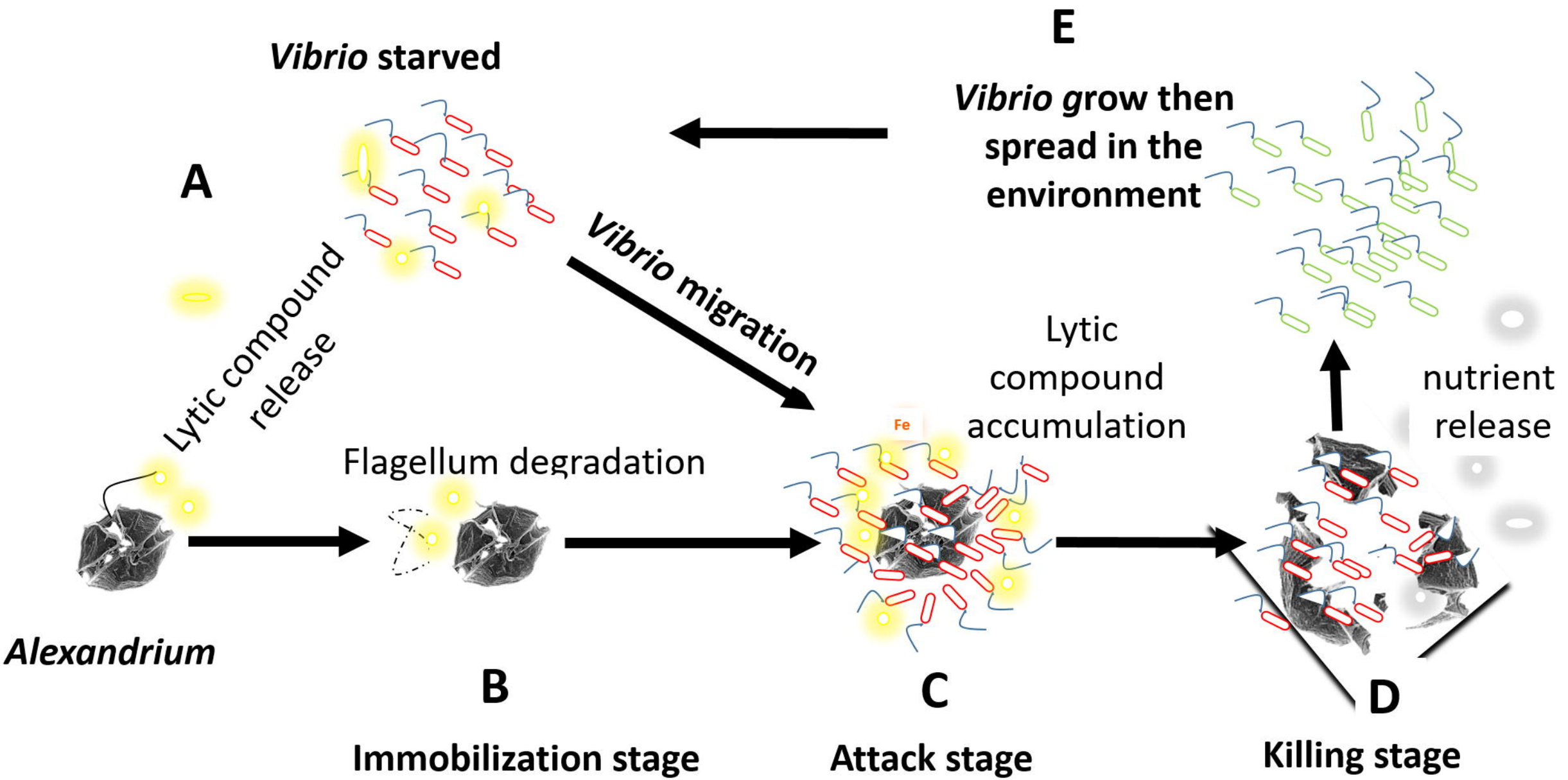
E
Vibrio starved
Vibrio grow then spread in the environment
A
Vibrio migration
Lytic compound release
Lytic compound accumulation
nutrient release
Fe
Flagellum degradation
Alexandrium
B
C
D
Immobilization stage
Attack stage
Killing stage

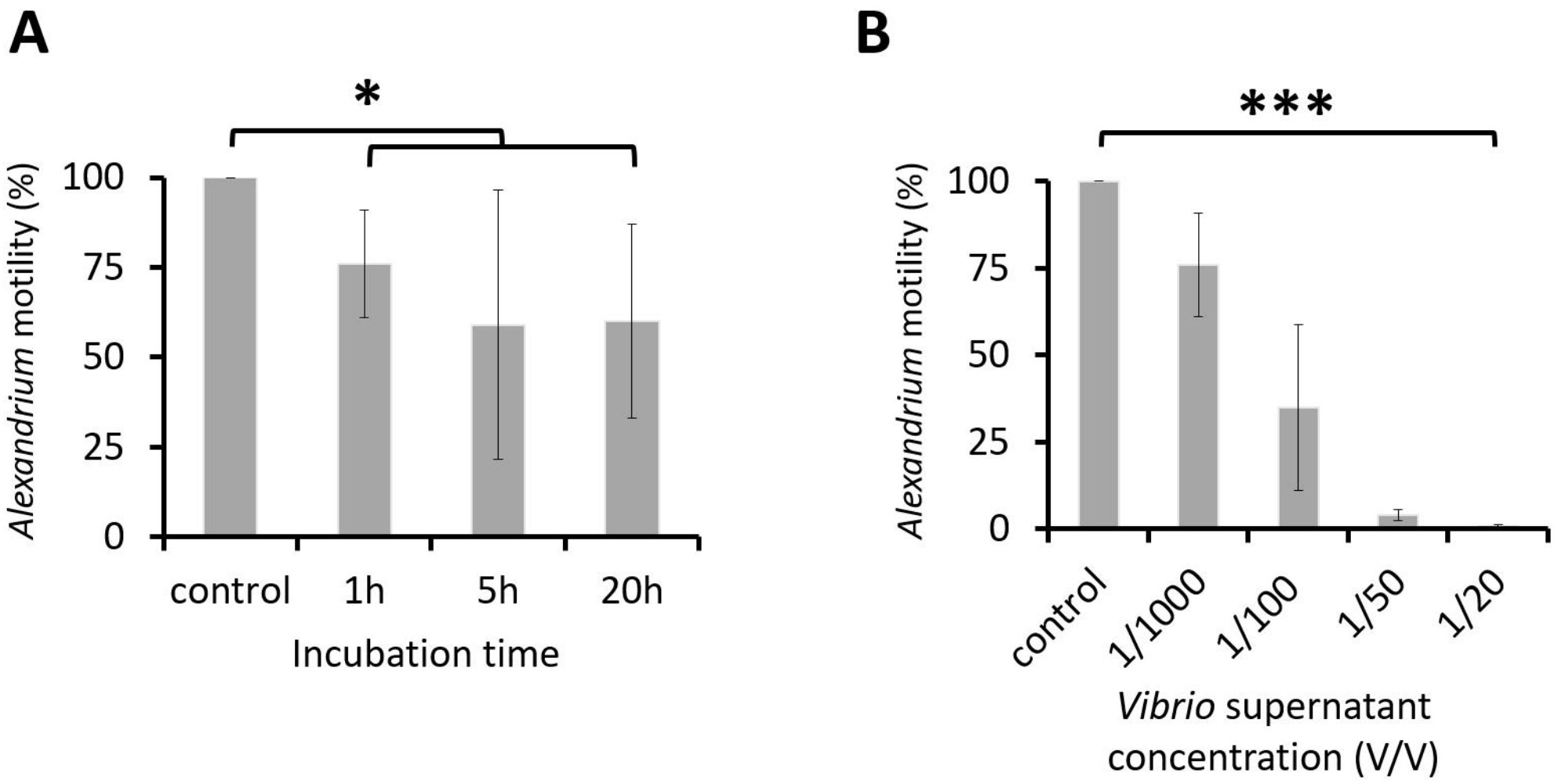
A
*
100
75
50
25
0
Alexandrium motility (%)
control
1h
5h
20h
Incubation time
B
***
100
75
50
25
0
Alexandrium motility (%)
control
1/1000
1/100
1/50
1/20
Vibrio supernatant concentration (V/V)

A

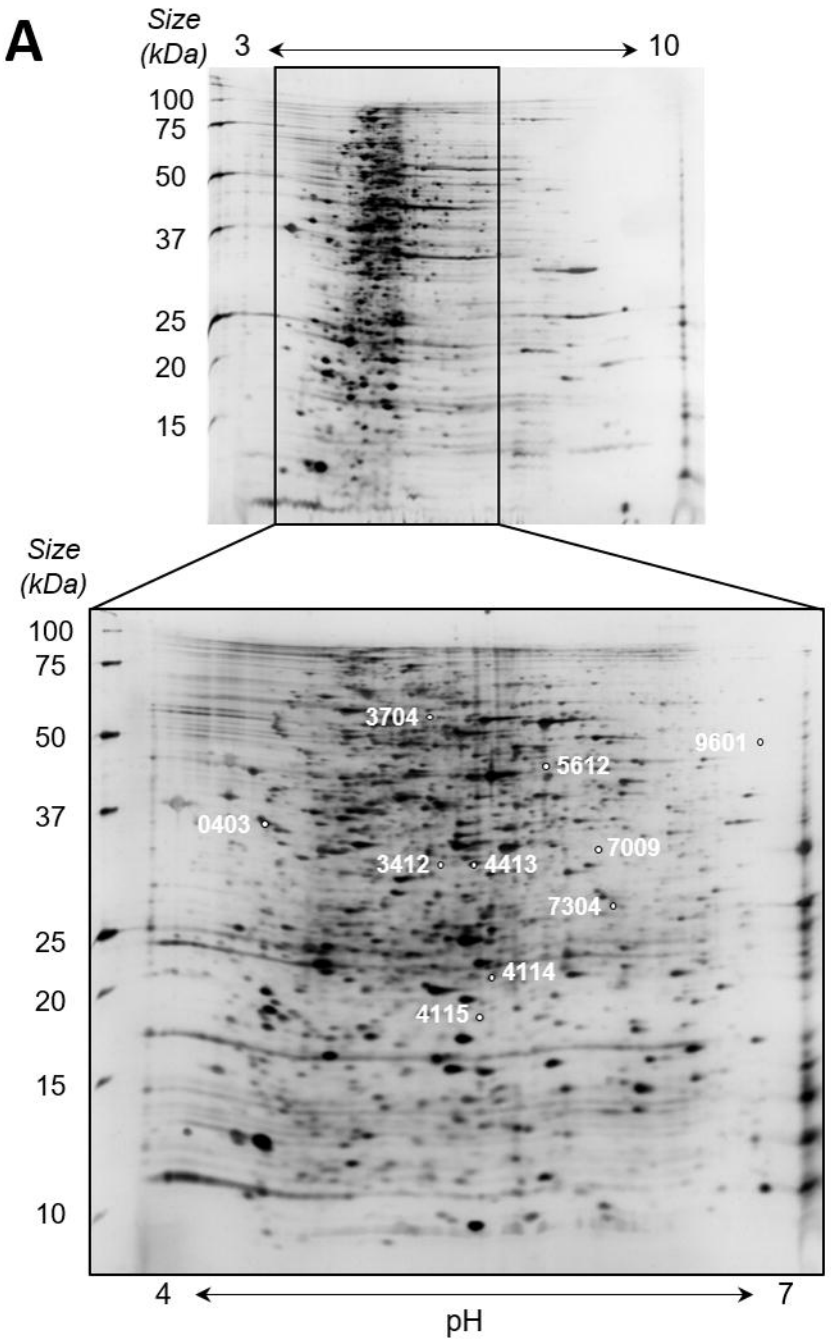

B

Spot #	Value ENSW	Value Zobell	Ratio (ENSW/Zobell)	Best ID Accession	#Peptides	-10logP Prot	-10logP Pept. Min	-10logP Pept. Max	Seq coverage	CDD accession	Best ID Description	Expected mass	Expected pI
7304	3620,4	570,7	6,34	WP_012601215.1	3	172,83	67,81	92,01	14%	PRK00443	glucosamine-6-phosphate deaminase	29610	5,53
4115	1203,8	191,9	6,27	ND									
0403	3697,4	750,2	4,93	WP_004733797.1	16	253,95	23,25	124,97	33%	cd13641	ABC transporter substrate-binding protein	36195	4,52
4413	**640,2**	**267,4**	**2,39**	**WP_012600975.1**	**21**	**241,28**	**25,81**	**101,45**	**51%**	**PRK11411**	**iron siderophore-binding protein, PvuB**	**36111**	**5,73**
7009	616,6	316,3	1,95	ND									
3704	683,2	1303	-1,91	WP_009848030.1	30	360,8	29,21	121,35	54%	PRK09344	phosphoenolpyruvate carboxykinase (ATP)	59755	4,85
4114	315,2	812,6	-2,58	WP_009847387.1	2	58,71	58,71	58,71	8%	PRK00129	uracil phosphoribosyltransferase	22658	5,21
3412	57,7	238,2	-4,13	WP_012604509.1	10	244,21	29,11	105,11	38%	cd13674	C4-dicarboxylate ABC transporter	36946	5,26
5612	211,4	1395,9	-6,60	WP_012600249.1	2	79,11	40,49	40,83	6%	PRK05451	dihydroorotase	37599	5,36
9601	76,9	1717,1	-22,33	WP_004736554.1	12	208,83	33,74	100,38	29%	PRK08722	beta-ketoacyl-(acyl-carrier-protein)synthase II	43007	5,95

A

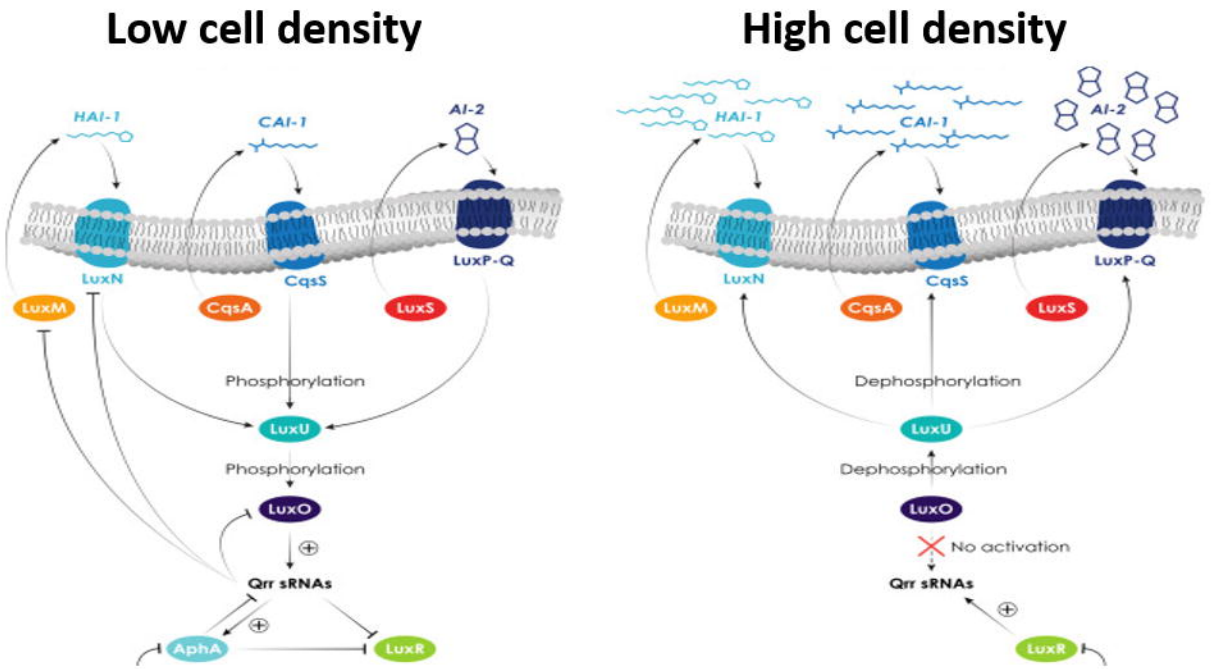
Low cell density
High cell density
HAI-1
CAI-1
AI-2
LuxN
CqsS
LuxP-Q
LuxM
CqsA
LuxS
Phosphorylation
LuxU
Phosphorylation
LuxO
Qrr sRNAs
AphA
LuxR
Dephosphorylation
Dephosphorylation
No activation

B

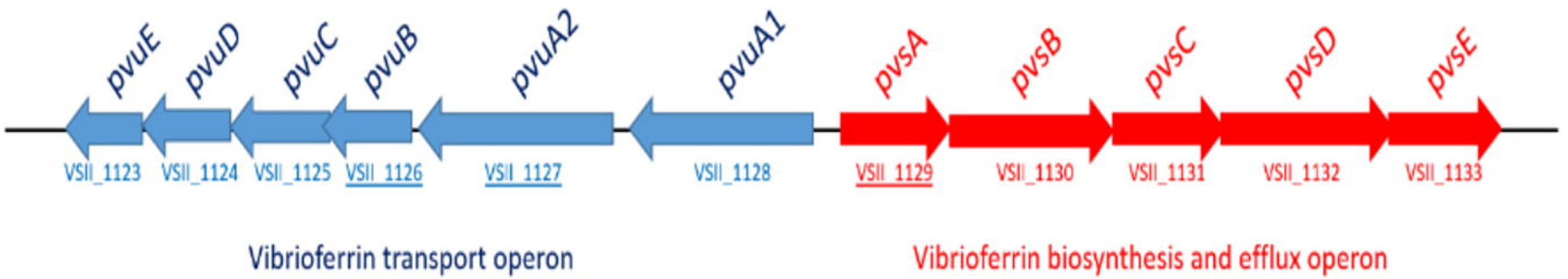
pvuE
pvuD
pvuC
pvuB
pvuA2
pvuA1
pvsA
pvsB
pvsC
pvsD
pvsE
VSII_1123
VSII_1124
VSII_1125
VSII_1126
VSII_1127
VSII_1128
VSII_1129
VSII_1130
VSII_1131
VSII_1132
VSII_1133
Vibrioferrin transport operon
Vibrioferrin biosynthesis and efflux operon